

Tarptautinė mokslinė-praktinė konferencija

**INOVACIJOS LEIDYBOS,
POLIGRAFIJOS IR MULTIMEDIJOS
TECHNOLOGIJOSE 2021**

Straipsnių rinkinys

International scientific-practical conference

**INNOVATIONS IN PUBLISHING,
PRINTING AND MULTIMEDIA
TECHNOLOGIES 2021**

Proceedings

Kaunas, 2021

Scientific committee

Ph.D. Professor Georgij Petriaszwili
(Warsaw University of Technology, Poland)
Ph.D. Professor Halina Podsiadlo
(Warsaw University of Technology, Poland)
Ph.D. Associate Professor Adem Ayten
(Istanbul Aydin University, Turkey)
Ph.D. Associate Professor Sergej Nikolaevich Ankuda
(Minsk State Higher Radiotechnical College, Belarus)
Ph.D. Associate Professor Kęstutis Vaitasius
(Kaunas University of Technology, Lithuania)
Ph.D. Professor Rimas Maskeliūnas
(Vilnius Gediminas Technical University, Lithuania)
Ph.D. Associate Professor Renata Gudaitienė
(Kaunas University of Applied Sciences, Lithuania)
Ph.D. Associate Professor Mehmet Oguz
(Marmara University, Applied Sciences School, Turkey)
Ph.D. Associate Professor Vilma Morkūnienė
(Kaunas University of Applied Sciences, Lithuania)
Ph.D. Associate Professor Svetlana Havenko
(Ukrainean Academy of Printing, Ukraine)
Ph.D. Associate Professor Renata Gudaitienė
(Kauno kolegija/University of Applied Sciences, Lithuania)
Ph.D. Associate Professor Daiva Sajek
(Kauno kolegija/University of Applied Sciences, Lithuania)

The articles are peer-reviewed

Articles are available on:

<http://ojs.kaunokolegija.lt/index.php/TMPK>

Contact information

Kauno kolegija / Kaunas University of Applied Sciences
Faculty of Technologies
Department of Media Technologies
Pramonės pr. 20, LT-50468 Kaunas, Lithuania

Contact person

Renata Gudaitienė
E-mail: konferencija.md@go.kauko.lt

CONTENTS

**Ginevičienė G., Gudaitienė R., Kujalavičius Ž.,
Lukaševičiūtė D., Pocienė A.**

INVESTIGATION OF THE EFFECT OF LASER RADIATION
ON THE MORPHOLOGY AND COLOUR
OF BIRCH PLYWOOD5

Kandirmaz E.A., Ozcan A.

THE USE OF ENCAPSULATED AMMONIUM POLYPHOSPHATE
IN THE PRODUCTION OF FLAME RETARDANT PAPER 21

Назар О. Р.

ИССЛЕДОВАНИЕ КАЧЕСТВА ОТТИСКОВ ТЕРМОТРАНСФЕРНОЙ ПЕЧАТИ
НА РАЗЛИЧНЫХ ТКАНЯХ 32

Ozcan A., Cidik E., Kandirmaz E.A.

THE EFFECT OF DIGITALIZATION ON ILLUSTRATION
IN GRAPHIC DESIGN 39

Юраскова И., Проскуряков Н.

КОМПЛЕКСНЫЙ ПОКАЗАТЕЛЬ КАЧЕСТВА ПЕЧАТИ
НА АЛЮМИНИЕВЫХ БАНКАХ 52

Sajek D., Valčiukas V.

STUDY OF IMAGE MICRO-LINES REPRODUCTION QUALITY
ONTO DIGITAL OFFSET PRINTING PLATES 58

Tutak D., Ozcan A., Kandirmaz E.A.

INVESTIGATION OF THE FLAME-RETARDANT PROPERTY
OF SILICA NANOPARTICLES RATIO
IN THE PAPER COATING 67

Васильев И.Ю., Ананьев В.В., Черная И.В.

БИОРАЗЛАГАЕМЫЕ МАТЕРИАЛЫ НА ОСНОВЕ ПЭНП,
КРАХМАЛА И МОНОГЛИЦЕРИДОВ 75

INVESTIGATION OF THE EFFECT OF LASER RADIATION ON THE MORPHOLOGY AND COLOUR OF BIRCH PLYWOOD

Ginevičienė G., Gudaitienė R., Kujalavičius Ž.,
Lukaševičiūtė D., Pocienė A.
Kaunas University of Applied Sciences

Abstract

CO₂ laser is commonly used for the production of the advertising material onto plywood, yet the final result of the product depends on the appropriate selection of material, its morphological properties, and technological parameters of material processing. As a result, the change in colour, the depth of the burnt plywood surface due to laser exposure and surface morphology is different. The paper presents the results obtained when the birch plywood is exposed to the CO₂ laser, which renders a specific colour change. The paper also discusses how morphological and roughness parameters influence the colour changes and which material processing mode is the best to achieve a desirable result.

Keywords: *engraving, gas CO₂ laser, glued plywood (fibreboard, birch plywood), ΔE colour change, surface morphology, ablation, carbonisation*

Introduction

In the course of the production of visual products, when a number of various finishing modes are commonly used, the final result of the product depends on the colour change ΔE and morphological properties of the material used. Therefore, it is very important to identify a link between these aspects and the technological parameters that affect them. To process plywood used for the advertising products, gas CO₂ laser is commonly used. The principle of laser beam operation is based on the effect of the concentrated laser beam, which destroys the surface structure of the material. With the help of these devices, computer-generated shapes are transferred onto materials with various morphological and colorimetric properties of the surface. Taking into consideration the selected parameters of laser operation mode, such as the intensity of laser beam and type of the material, different tones of colour of the drawn objects can be obtained (Varanavičienė et al., 2017).

Change in colour can be affected both by the type of wood, laser power, speed of movement, thickness of the material and energy flow density (Petru et al., 2014). Carbonisation process occurs when wood is engraved using a laser. The depth of carbonised wood corresponds to the width of fibre (Dogaru, 1985, cited from Petru et al., 2014). As a result, different intensities of ash colour and brownish colour tones are obtained on the burnt wood surface (Kuktaitė et al., 2020a). Differences in the colour tone of graphic images are obtained as the surface of the material is exposed to different laser power and its movement speed. The colour changes become more pronounced as the speed of laser beam movement decreases, accordingly. An increase in moisture content reduces the effect of carbonisation, as the excess of energy is used for the vaporisation process from wood (Petru et al, 2014). It was observed that the sharpest contrast is obtained when alder, birch and maple plywood is exposed to laser beam radiation.

Plywood is widely used to transfer visual and textual advertising information. Plywood is environmentally friendly, easy to recycle and cost-effective material suitable for the production of products where laser engraving is applied (Kuktaitė et al., 2020a). Regardless of a large supply of wood materials available for engraving in the market, yet not all wood is suitable, as the quality and the final result depends on the type of wood, its physical and mechanical properties, in particular. Thus, an appropriate selection of the individual parameters of wood processing according to the type of board plays a vital role aiming to achieve a desirable result. Barnekov et al. (1986) claim that one of the major factors that determines laser and wood interaction is the nature of the wood chips, its density, moisture content, separated concentrated materials and optical properties (Gurau et al., 2017). CO₂ laser-adapted plywood is usually made from birch wood, which is resistant to atmospheric effects, and maintains the stability of properties under the influence of various external factors. Birch plywood consists of several high-quality full-sized veneer sheets of birch wood glued together. The sheets are glued with strong glues so that the texture of the adjacent layers is in an opposite direction. High temperatures and high pressure are used in the production of the plywood (Varanavičienė et al., 2017). Plywood is a strong and hard (robust) material, resistant to deformation and abrasion, with properties superior to ordinary wood. Its surface fibres are smoothed, there are no obvious defects in the wood structure, texture is uniform without additional contrasting shades of the surface, so when engraving a larger area, a more uniform solid colour tone is obtained. However, various patterns of wood present in the glued plywood do not allow to achieve 100 % uniform colour tone over the entire area of the object,

but due to the smoothness of the plywood surface, more intense and more uniform colour tones of different intensity are obtained in comparison to homogenous structure of fibreboard.

The quality of engraving depends on the thickness of wood, density, moisture content and glue (Petru et al 2014). Petru et al. (2014) found in the study that a low laser power cannot pass through the entire thickness of wood plywood, whereas a high laser power burns the wood. Laser used for the wood processing darkens the colour of the plywood surface, as the colour may range from light brown to black. Lin et al. (2008) investigated the effect of movement speed ratio and laser radiation power on the depth and colour difference of the MOSO® bamboo laminate and found that the higher power of radiation and lower speed of movement, the higher values in colour difference and the greater depth (cited from Gurau et al., 2017). The study showed that the above-mentioned factors can be predicted and evaluated by regression analysis. Li et al. (2020) state that the principles of laser beam operation such as laser power, movement speed and radiation width have a significant effect on the colour components ΔL and ΔE of bamboo surface. Absolute values increased in the presence of a higher laser power, but decreased with increasing speed of laser beam movement and operating range. The relationship between laser beam operating parameters and colour digital coordinates ΔL and ΔE was determined. This method can be applied in order to achieve a desirable colour or different colour choices (Li et al., 2020). Based on the study carried out by G. Kuktaité et al. (2020b), it was found that in the presence of different parameters of laser beam speed and radiation power, samples of close colour tones on birch plywood can be obtained, e.g. differences in ΔE values do not exceed 3, which corresponds to the limits of the imperceptible colour difference of the observer's visual assessment. It was also found that the power of laser radiation has a greater effect on the changes of colour properties of wood plywood than movement speed. The value of ΔE is proportional to the laser radiation power, given the laser beam moves at a maximum speed of 600 mm/s. The value obtained in the samples was the lowest, as a laser beam moved faster through the sample width. The highest ΔE value was obtained when the lowest speed was chosen, as a laser beam moved at a lower speed, and the microstructure of wood plywood exposed to a laser beam for a longer period was more damaged (G. Kuktaité et al., 2020b).

Irawan et al. (2008) investigated how CO₂ laser creates (destroys) microstructures due to the mechanism of photothermal ablation. It was found that a 10,6 μm laser beam is absorbed by fibrous materials, later on, heats, melts and vaporises them. Due to this process applied, a void is left on the wood.

The depth of microstructures is determined by the properties of material, the power of laser radiation, the number of the laser passes and the speed of movement of the laser beam. The depth of microstructure linearly depends on the set of parameters of the laser beam, yet the laser power has to be optimised taking into consideration properties of the material (Klank et al., 2002, cited from Irawan et al., 2008). A study by Gurau et al. (2017) found a correlation between change in colour of wood (difference in colours measured by ΔE) and surface roughness (measured roughness parameters R_a , R_q , R_t , R_k , R_{pk} , R_{vk}). Such correlations can be useful in selecting power and speed combinations that can provide the minimum surface roughness for the selected colour change (Gurau et al., 2017). Gurau et al. (2017) claim that roughness of the surface and total colour difference ΔE increased with laser power and decreased with the scanning speed, respectively. When the speed was higher than 300 mm/s, a slight difference in colour was observed, whereas surface roughness remained the same (Gurau et al., 2017). Pritam (2016) found that the arithmetic roughness average R_a decreases as movement speed and laser power increases. To reach deeper cavities, but at a lower speed, it is recommended to increase the frequency of laser scanning at lower power and higher speed of movement (Pritam, 2016).

Based on the study carried out by G. Kuktaitė et al. (2020a), the analysis of the ΔE results showed, that the change of laser technological parameters has an effect on colorimetric indices of the plywood and processes of laser ablation, as a deep graphic image is obtained in a material with different morphological properties. In the overview on laser engraving done by Patel et al. (2015), the influence of process parameters including laser power scanning speed and laser frequency on engraving and surface roughness is emphasized (Gurau et al., 2017). As noted in the article, information on the effect of different laser technological parameters on the morphological properties of the material surface, radiation ablation processes, set of the concentrated laser beam parameters that destroys the structure of material surface and application of clearly defined visual production is insufficient.

Based on the aforementioned data, it can be stated that the selection of optimal parameters of technological processes becomes a key issue when transferring the computer-generated image onto the plywood. Thus, the aim of this study is to analyse the effect of technological parameters of CO_2 laser radiation (power and speed) on the morphology of the glued birch plywood and colour, and to determine the correlation between ΔE and R_a parameters, applying the method of morphological metrology and the comparative spectrophotometric analysis of surface colour tones.

Methodology

A vector layout was developed using Adobe Illustrator software. The layout was imported into RDWorks V8 computer software, which has an interface with Bodor BCL-MU CO₂ laser, used for engraving objects. Laser beam operating field corresponded to the size of the chosen objects. Bodor BCL-MU CO₂ laser with a beam wavelength of 10.6 µm and an engraving speed of 0–60000 mm/min. Minimum engraving area of 1 mm × 1 mm. To ensure an appropriate operating environment of the device, 18 °C room temperature and 41 % humidity was maintained (Bodor User Manual for BCL-MU Series Laser Machine, 2019).

In this study, a birch plywood sheet of 500 × 300 mm specially adapted for cutting and engraving was chosen for the analysis. Composition and parameters of the analysed sample: 100 % birch, 3 mm of thickness, rigid thickness tolerance of plywood (+0,3 / –0,3), density 640–700 kg/m³, high-quality full-size veneer inside and outside, a minimum number of defects in all layers. Based on the measurements carried out by G. Kuktaité et al. (2020a), specific areas of the sample affected by the combination of power and speed parameters were selected for a more detailed analysis. The analysed area of the sample consisted of a number of 18, 50 × 50 mm sections exposed to laser radiation. To carry out an analysis, appropriate combinations of power and speed of 20 % 200 mm/s, 20 % 240 mm/s, 100 % 600 mm/s were selected. In the samples, marked 200v, 240v and 600v, changes in colour tones and microstructure of the plywood surface were observed.

For the analysis of change in colour tones, X-Rite I1 Pro spectrometer was used to carry out measurements. The measurement data are presented as the change in ΔE in compliance with ISO/CIE 11664-4:2019 standard (Lithuanian Standards Board, 2019). Standard ISO/CIE 11664-4:2019 regulates a mathematical formula for estimating the change in colour between two objects compared. The value of ΔE determines the change between L*a*b* coordinates corresponding to the position of colour tones in the colour space. The values of ΔE for visual assessment are regulated by the standard. The result of the observer's visual assessment depends on the ΔE value of the digital colour coordinate difference. Given $\Delta E < 3$, the difference in colours is almost imperceptible. When $3 \leq \Delta E \leq 6$, difference in colours is observed, when two objects are adjacent. When $\Delta E > 6$, colour difference is visible by the naked eye, and when the value increases, a significant colour contrast is observed. Colour measurements were performed at five points on the sample.

Roughness can be considered as a major criterion describing the quality of the treated surface, since it determines further methods of surface fin-

ishing, possible application and appearance. The values of surface roughness are regulated by the standard 4287:1997. The standard covers main indicators as follows: the arithmetic average of the profile deviations R_a , the average roughness R_z , etc. (Baskutis et al., 2019). The arithmetic average of the absolute values of the profile roughness R_a and the height of micro-roughness R_z were evaluated in three directions of wood fibre: along the wood fibre, across the wood fibre, and at an angle of 45° , measured at five points. The profilometer PCE-RT 1200 was used to determine the surface morphology of the birch plywood. The profilometer operates according to the touch method in accordance with ISO 3274. The RC wave filtering method was chosen, setting an expected marginal length 2,5 mm, measuring zone 10 mm.

The quality of the structural properties of plywood was evaluated by capturing images using Invenio 5SII camera with the installed optical microscope Motic SMZ-171. The surface image of the analysed sample was magnified $2 \times 2 \times 10$ times with a resolution 2560×1922 pixels. Live image speed is up to 48 fps. The 3D optical system MicroCAD Lite was used to record deformations of the surface and obtain precise classification results (see Fig.1). The distance to the measured surface of the sample (object) was 3 cm, resolution $0,1 \mu\text{m}$, measurement resolution 748×480 pixels, and the measurement zone covered $1,8 \times 1,2$ mm area. The 3D MicroCAD optical system works with ODSCADGFM 3D measurement and analysis software. The relief of the sample surface was scanned with the camera and the 3D photograph was taken. The selected optical scanning methods allowed to determine a more precise microstructure of the plywood surface.

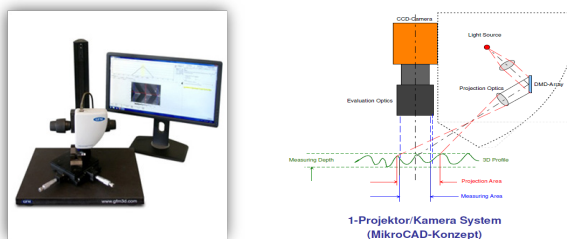


Fig.1 Optical 3D MicroCAD Lite measurement device and projector/ camera system (MicroCAD concept)(Lmi technologies, 2021)

Result analysis

Birch plywood was treated with a gas CO_2 laser by selecting different parameters (Fig.2). The power and movement speed of the laser beam were

selected based on the colour tone palette developed by G. Kuktaité et al.(2020a), designed to determine the value differences of colour tones on plywood, when the value differences correspond to $\Delta E < 3$ limits. The colour differences of the samples obtained by selecting the following laser speed 600 mm/s and 100% power (600v), speed 200 mm/s (200v) and 240 mm/s with 20% power (240v), were insignificant. Yet, the effect of laser applying such technological parameters on the morphological properties of the plywood surface was unknown. With the increasing laser speed and power, a smoother surface of the plywood is obtained, thus a combination of 600 v technological parameters was chosen as the reference sample (Table1).

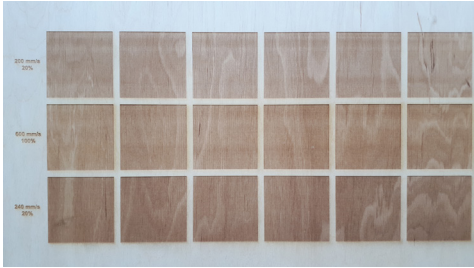


Fig.2 Samples of birch plywood after exposure to radiation

The effects of radiation power and beam speed were analysed using a spectrophotometric method. The difference in colour tones between radiation-exposed samples and unaffected plywood was evaluated by ΔE vector values of digital colour coordinate differences, presented in Table 1. The table shows five ΔE arithmetical averages of six engraved samples on the plywood, where the average of the averages is derived and the difference of the averages of 200v, 240v and 600v is calculated.

Table 1. Colour difference ΔE on glued plywood exposed to radiation

Process	Laser parameters		ΔE difference, sample						ΔE	
	Speed, mm/s	Power, %	1	2	3	4	5	6	Average	Difference between 600v
Plywood	Unaffected	Unaffected	1,15	1,06	0,74	1,2	1,58	0,84	1,1	25,7
200v	200	20	25,78	25,17	22,4	24,19	24,67	24,25	24,41	2,39
240v	240	20	28,89	27,99	28,38	27,39	28,73	29,17	28,43	1,63
600v	600	100	26,17	26,19	25,17	27,37	27,4	28,52	26,8	0

Having analysed the obtained ΔE values, it was observed that the change of technological parameters affects the colorimetric indices of the plywood surface. The ΔE value differences are insignificant and fall within the imperceptible limits of the observer's visual assessment, e.g. $\Delta E < 3$, but their differences indicate that the speed of beam movement had an effect on the colour tone of the plywood surface. The average value of ΔE obtained at a speed of 240 mm/s for laser beam was 16% higher than moving at the speed of 200 mm/s, yet compared to the average value of ΔE at the speed of 600 mm/s, the difference of the ΔE value average is 0,76 smaller than between the 200v and 600v samples. Figure 3 presents values of the average differences that confirm that the difference in colour tones is smaller between the 600v and 240v samples.

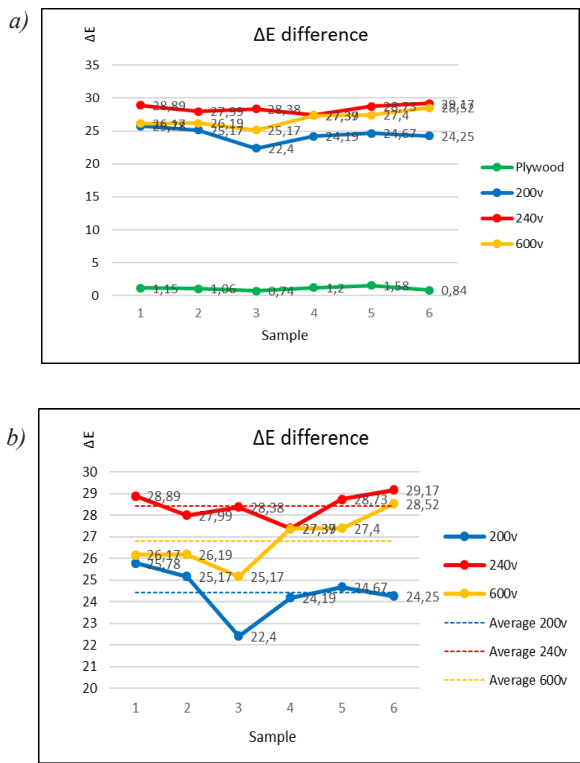
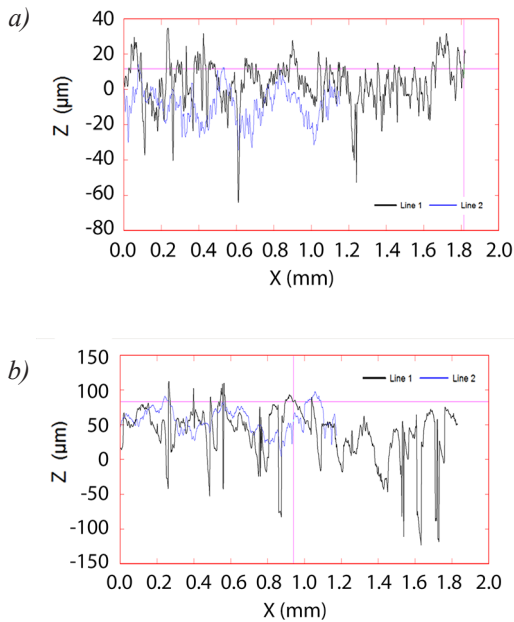


Fig 3. Colour difference ΔE on glued plywood exposed to radiation:
a) ΔE change in plywood affected and unaffected by laser b) ΔE average values

The metrological study method of surface morphology was used to compare structural surface properties of laser-untreated glued plywood with the different parameters affected by engraving process on the fibreboard samples. In addition, the maximum changes in the height of micro-roughness R_z and the arithmetic means R_a of the profile roughness R_a were determined. The data of arithmetic means obtained in the study are given in Table 2.

In the course of the study, it was observed that the speed of beam movement and radiation power influenced the ablation process. Comparing the surface of the unaffected plywood with the surface that was affected by the combination of laser technological parameters, the increase in the values of roughness indices R_a and R_z was insignificant in transverse, longitudinal and 45° angle wood fibre directions in the glued, laser-exposed plywood. The lowest roughness was found in 600 v samples affected by a combination of laser parameters, the highest roughness in 200 v samples, whereas data values of 200 v samples were close to the values of 600 v samples. Figure 7 shows how the surface roughness of fibreboard alters during the laser engraving process in the longitudinal and transverse directions of wood fibre.



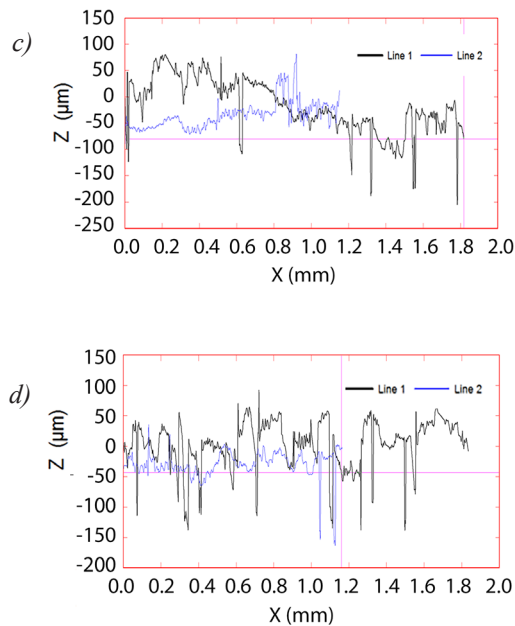


Fig. 4 Difference in roughness in the longitudinal and transverse direction of the plywood fibre

a) Unaffected plywood, b) 200v sample, c) 240v sample, d) 600v sample

Percentage values are used to determine the increase in roughness. Comparing plywood exposed to 20 % radiation power, but with a beam moving at different speeds (200 mm/s and 240 mm/s), it was determined an insignificant, yet greater effect of speed on morphological surface properties, e.g. in the 200v samples, when a laser beam was exposed in the longitudinal direction of wood fibre, the arithmetic average values R_a are 1,2 % higher, corresponding to the absolute difference 0,12 μm , whereas R_z values are 1,4 % higher (absolute difference 0,38 μm); in the transverse direction of wood fibre R_a – 10,6 % (absolute difference 1.51 μm), R_z – 10.9 % (absolute difference 4.4 μm) higher. This proves that a smoother surface of plywood was obtained at 6,7 % higher speed (240 mm/s).

Table 2. Morphology of plywood surface after exposure to radiation


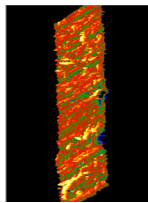
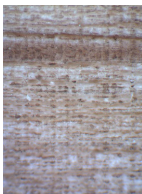
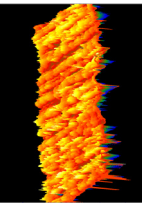
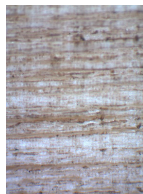
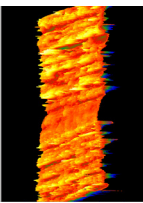
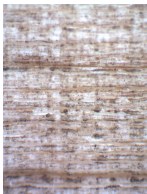
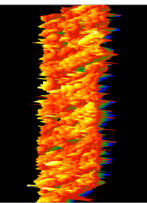
Process	Microscopic image	3D Microscopic image	Ra, μm			Rz, μm		
	Structure of glued plywood	Morphology of plywood surface	Along the wood fibre	Across the wood fibre	45° angle	Along the wood fibre	Across the wood fibre	45° angle
Unaffected plywood			2,08	5,41	5,33	5,89	15,28	15,05
200v- 200 mm/s, 20%			9,84	15,83	14,17	27,88	44,81	40,09
240v- 240 mm/s, 20%			9,72	14,32	14,87	27,50	40,41	42,06
600v- 600 mm/s, 100%			9,65	13,78	15,33	27,28	38,97	43,36

Table 3. Comparison of the increase in surface roughness of fibreboard between 200v and 240v samples after exposure to radiation

Indices	Surface roughness					
	Along the wood fibre			Across the wood fibre		
	200v, μm	240v, μm	Increase, %	200v, μm	240v, μm	Increase, %
Ra	9,84	9,72	1,24	15,83	14,32	10,55
Rz	27,88	27,50	1,38	44,81	40,41	10,89

The obtained values of the surface roughness in the 200v and 240v samples are very close to the selected reference sample of 600v, it can be stated that the surface morphological data between the 240v samples and the reference sample differ the least in the longitudinal direction, when Ra – 0.7% (absolute difference 0.07 μm), Rz – 0.8% (absolute difference 0.22 μm), in the transverse direction Ra – 3.9% (absolute difference 0.54 μm), Rz – 3.7% (absolute difference 1.44 μm). The speed of beam movement varied by 60% in the samples, radiation power by 80%, yet technological parameters of laser operation did not have a significant influence on the changes in the results obtained.

Table 4. Comparison of the increase in surface roughness of plywood in 200v, 240v and 600v samples after exposure to radiation

Indices	Surface roughness						Surface roughness					
	Along the wood fibre			Across the wood fibre			Along the wood fibre			Across the wood fibre		
	200v, μm	600v, μm	Increase, %	200v, μm	600v, μm	Increase, %	240v, μm	600v, μm	Increase, %	240v, μm	600v, μm	Increase, %
	200v, μm	600v, μm	Increase, %	200v, μm	600v, μm	Increase, %	240v, μm	600v, μm	Increase, %	240v, μm	600v, μm	Increase, %
Ra	9.84	9.65	1.97	15.83	13.78	14.88	9.72	9.65	0.73	14.32	13.78	3.92
Rz	27.88	27.28	2.2	44.81	38.97	14.99	27.50	27.28	0.81	40.41	38.97	3.7

Having analysed the general data on changes in colour tones and surface roughness, the best correlation was observed between the analysed samples. It was found that the average values of ΔE and surface roughness of the 600v correlate with 240v sample parameters, when the samples are exposed to a combination of laser parameters. Thus, it can be stated that 600v samples correlate with 200v samples, but the differences in the obtained values in the 600v sample are larger than in 240v samples.

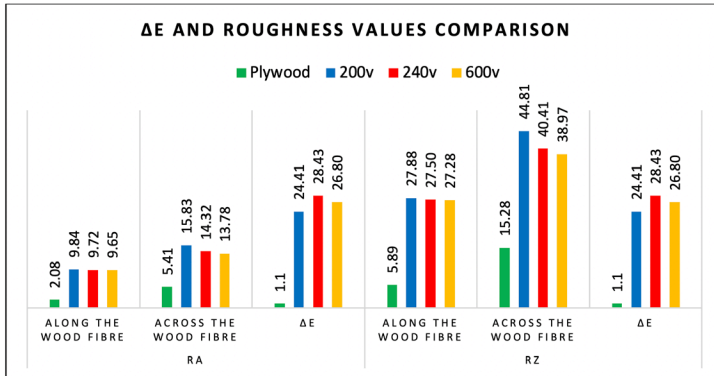


Fig.5.Comparison of average values between ΔE and surface roughness

Consequently, in the production of visual objects using laser engraving technology, and in order to obtain the desirable colour tone in glued plywood, different combinations of technological parameters of laser operation (radiation power, speed of laser beam movement) can be applied, ensuring optimal reduced surface roughness of the material. The study showed that the average values of ΔE with a minimum difference in morphological properties were obtained using combinations of technological laser parameters applied onto 600v and 240v samples, corresponding to the limits of the small range of $25 \leq \Delta E \leq 30$ colour change. It can be claimed that the minimum occurrence of roughness is proportional to the minimum change in colour tone. However, the 600v sample was produced using 100% laser power, whereas the 240v sample 20% laser power. Considering the speed of laser movement and the amount of energy consumed, it can be stated the production of the second sample required a lesser amount of energy consumption, while the colour obtained of the latter sample was analogous ($\Delta E < 3$) to the sample produced at a higher speed.

This study can be further developed to investigate the influence of radiation on the structural properties of the finishing processes, the shape of graphic objects of different areas and their combinations, compatibility with other printing technologies, and processes of the material ablation. Based on the obtained results, certain proposals can be made for the production of graphic objects, taking into consideration the proportions of time and CO_2 laser gas consumption and selection of a more efficient production method.

Conclusions

1. Changes in the technological parameters of laser affect the colorimetric indices of the surface of glued plywood. Insignificant differences in ΔE were obtained fall within the imperceptible limits of the observer's visual assessment, e.g. $\Delta E < 3$, but their differences indicate that the speed of the beam movement influenced the colour tone of the fibreboard.

2. Comparing the surface of the laser-affected surface of the plywood with the surface that was exposed to the combination of the technological laser parameters, it was found, that the values of surface roughness R_a and R_z , increased by 2.7 time in the transverse direction of wood fibre, 4.7 times in the longitudinal direction, and 2.8 at 45° angle, accordingly.

3. The minimum change in the movement of the laser beam has an impact on the morphological properties of glued plywood surface. The increase in the speed of laser beam by 6.7% had a smaller effect on the ablation process, as the obtained microstructure of plywood surface was smoother 1.2% in the longitudinal direction, in comparison to 10.6% in the transverse direction.

4. The average values of ΔE that correspond to the visual assessment requirements of the observer (when $\Delta E < 3$) were obtained with a minimum difference of morphological properties, when appropriate combinations of technological parameters of laser beam 600v and 240v. Given $\Delta E=1,63$ change, the smallest difference in the morphological indices of the surface is obtained, when $R_a - 0,7\%$ and $R_z - 0,8\%$ in the longitudinal direction, and $R_a - 3,9\%$ and $R_z - 3,7\%$ in the transverse direction. This determines the choice of parameters depending on the laser power consumption.

5. To obtain the desirable colour tone in the glued plywood, different combinations of technological parameters of laser operation (radiation power, speed of laser beam movement) can be applied in the production of visual objects, by means of laser engraving technology, ensuring optimal surface roughness of the material. The minimum roughness is proportional to the minimum change in colour tone, when plywood is processed at 240 mm/s speed and 20% power, and at 600 mm/s and 100% laser power.

Literature

1. Baskutis, S., Rimša, G. (2019). *Industry challenge 4.0 empowering metalworkers for smart factories*. Erasmus+ Program KA2: Cooperation for innovation and the exchange of good practices – Sector Skills Alliances. Project No. 575813-EPP-1-2016-1-LT-EPPKA2-SSA [seen 20-09-2021]. Access online: https://ec.europa.eu/programmes/erasmus-plus/project-result-content/7fdbbe34-6aee-4fa6-99a2-473d9bb0dc4d/wp3_textbook_en.pdf

2. Barnekov, V. G., McMillin, C. W., & Huber, H. A. (1986). Factors influencing laser cutting of wood. *Forest Products Journal* 36 (1): 55-58.
3. Bodor User Manual for BCL-M Series Laser Machine (2019). Jinan Bodor CNC Machine Co.Ltd
4. Dogaru, V. (1985). Bazele tăierii lemnului și a materialelor lemnoase. Basics for cutting wood and wood-based.
5. Gurau, L., Petru, A., Varodi, A., & Timar, M. C. (2017). The influence of CO₂ laser beam power output and scanning speed on surface roughness and colour changes of beech (*Fagus sylvatica*). *BioResources*, 12(4), 7395-7412.
6. Gurau, L., & Petru, A. (2018). The influence of CO₂ laser beam power output and scanning speed on surface quality of Norway maple (*Acer platanoides*). *BioResources*, 13(4), 8168-8183.
7. International Standard ISO 12647-2:2013. Graphic technology – Process control for the production of half-tone colour separations, proof and production prints. Part 2: Offset lithographic processes.
8. Irawan, R., Chuan, T. S., Meng, T. C., & Ming, T. K. (2008). Rapid constructions of microstructures for optical fiber sensors using a commercial CO₂ laser system. *The Open Biomedical Engineering Journal*, 2, 28.
9. ISO/CIE (2019). Publication 11664-4:2019. Colorimetry–Part 4: CIE 1976 L*a*b* Colour Space. CIE International Commission on Illumination. Available online: <https://www.iso.org> (accessed on 6 September 2021).
10. Klank, H., Kutter, J. P., & Geschke, O. (2002). CO₂ laser micro-machining and back-end processing for rapid production of PMMA-based microfluidic systems. *Lab on a Chip*, 2(4), 242-246.
11. Kuktaité, G., Cirtautaitė, G., Dubickaitė, S., and Ginevičienė, G. (2020a). Lazerio parametrų įtakos medienos paviršiaus struktūros kokybei analizė. Inovacijų taikymas technologijose 2020: respublikinė mokslinė-praktinė studentų konferencija, 2020 m.: straipsnių rinkinys. Kauno kolegija. Technologijų fakultetas, 176-184.
12. Kuktaité, G., Cirtautaitė, G., Dubickaitė, S., and Ginevičienė, G. (2020b). Medienos spalvos pokyčių analizė po graviravimo lazeriu. Inovacijų taikymas technologijose 2020: respublikinė mokslinė-praktinė studentų konferencija, 2020 m.: straipsnių rinkinys. Kauno kolegija. Technologijų fakultetas, 193-199.
13. Li, R., Chen, J., & Wang, X. A. (2020). Prediction of the color variation of MOSO ® bamboo during CO₂ laser thermal modification. *BioResources*, 15(3), 5049-5057.

14. Lin, C. J., Wang, Y. C., Lin, L. D., Chiou, C. R., Wang, Y. N., & Tsai, M. J. (2008). Effects of feed speed ratio and laser power on engraved depth and color difference of MOSO® bamboo lamina. *Journal of Materials Processing Technology*, 198(1-3), 419-425.
15. Lmi technologies. *Optical 3D measuring instrument MikroCad* [seen 31-09-2021] Access online: <https://lmi3d.com/brand/mikrocad/>
16. Patel, S., Patel, S. B., & Patel, A. B. (2015). A review on laser engraving process. *JSRD-International Journal for Scientific Research and Development*, 3(1), 247-250.
17. Petru, A., & Lunguleasa, A. (2014). Wood Processing by Laser Tools. *International Scientific Committee*, 213.
18. Pritam, A. (2016). Experimental investigation of laser deep engraving process for AISI 1045 stainless steel by fibre laser. *International Journal of Information Research and Review*, 3(1), 1730-1734.
19. Schechtel, F., Reg, Y., Zimmermann, M., Stocker, T., Knorr, F., Mann, V., & Schmidt, M. (2016). Pulsed laser processing of paper materials. *Physics Procedia*, 83, 46-52.
20. Stepanov, A., Saukkonen, E., & Piili, H. (2015). Possibilities of laser processing of paper materials. *Physics Procedia*, 78, 138-146.
21. Varanavičienė, E., Domskienė, J., Jucienė, M., (2017). CO₂ lazerio parametų įtaka mechaninėms tekstilės medžiagų savybėms ir gaminio kokybei. *Jaunųjų mokslininkų konferencija: Pramonės inžinerija – 2017* (p. 197-202). Kaunas KTU.

THE USE OF ENCAPSULATED AMMONIUM POLYPHOSPHATE IN THE PRODUCTION OF FLAME RETARDANT PAPER

Kandirmaz E.A., Ozcan A.

Marmara University, School of Applied Sciences

Abstract

Papers have extreme burning and ignition properties due to their natural extracts. Today, it has become a necessity to provide late flammability properties to valuable papers such as money, checks, promissory notes. It is desired that the additives used to provide late flammability materials do not emit harmful gas. In this sense, the use of additives containing phosphate is increasing. Encapsulation allows a material to be protected by natural effects or to be dispersed more homogeneously in the dispersion medium. In this study, ammonium polyphosphate, known for its flame retardancy property, was encapsulated with an easy method and it was investigated whether it provides a late flammability feature on papers.

For this purpose, microencapsulated ammonium polyphosphate was prepared by in situ polymerization with glycidyl methacrylate (GMA) and polyurethane as the shell material, respectively. The chemical structure of microcapsules illuminated with Fourier transform infrared spectroscopy (FTIR), and size of microcapsules were determined with scanning electron microscopy (SEM). Paper coating formulations containing starch binder and encapsulated ammonium polyphosphate in different ratios (0,1,3,5,7,5) were prepared and coated onto office paper. Color (with spectrophotometer), gloss (with glossmeter), contact angle (with goniometer) and flame retardancy (with LOI) properties of coated papers were measured. Offset test prints were made on the coated papers produced with IGT C1 and the changes in color and gloss of the coating were determined. As a result, ammonium polyphosphate was successfully encapsulated by in situ polymerization. It was concluded that as the amount of microencapsulated ammonium polyphosphate increased, the flame retardancy property increased and there was no decrease in printability.

Keywords: Coating, Printability, Microcapsulation, Ammonium polyphosphate, Flame retardancy

Introduction

In the paper industry, as in other industries, circular production and biocompatibility is an increasingly important concept. It is expected that the environmental effects of the new features brought to the paper will be at the lowest level with the continuous increase in the desired features from paper. Some of the properties required from paper can be listed as smooth surface properties, printability, gloss, mechanical resistance properties, and resistance to heat and moisture. Recently, the importance of fire-resistant papers has been increasing especially in valuable papers, librarianship and wallpapers. Although the flame-retardant feature is not new in paper or polymer-based materials, this feature is traditionally gained with toxic substances that have environmental effects. Two methods can be used for flame retardant property in papers (Li and Wu, 2012). The first method is to add a flame retardant to the formulation in paper production. However, homogeneous distribution is very important in this method, otherwise it will not gain flame retardant property and there may be other problems (Ozcan et al., 2020). In addition, in this method, it functions as a flame retardant filler and causes printing problems by negatively affecting the flexibility of the paper. The second method is to make a single or double-sided coating on the paper. Besides being a very practical method, since a very thin film layer is applied to the surface, it does not cause problems in flexibility and printing problems do not occur.

Microencapsulation is a rapidly developing and growing technology that is being used in many sectors today. It can be defined as the coating of a material with a uniform film in the form of microparticles. Microcapsules consist of two parts, the core and the shell. The core consists of an active substance that can be solid, liquid or gas, while the shell protects the core material and is made of natural or synthetic polymers. The purpose here is to keep the core material in a suitable shell, to protect it from some environmental effects, and to extend its usage or durability life (Kandirmaz et al., 2020).

In recent years, there are studies showing that many polymers such as polypropylene, polyethylene, acrylonitrile butadiene styrene and Nylon 6 are used as flame retardants (Xia et al., 2008; Xie et al., 2006; Venkatram et al., 2018; Bee et al., 2018; Rezvani Ghomi et al., 2020). Ammonium polyphosphate (APP) is a material with a high phosphorus content that yields phosphoric acid, N₂ and ammonia when heated. Therefore, it can be used for flame retardancy of many organic polymers (Qu et al., 2014).

Material and Methods

Materials

Ammonium polyphosphate, cyclohexane, glycidyl methacrylate, benzoyl peroxide and butanone were purchased from Sigma-Aldrich, Germany. Starch was obtained from Merck, Germany. Process magenta ink was purchased from TOYO ink Co., Turkey. In this study, 80 g/m² office papers were used for coatings. Papers were obtained from UPM, Finland.

Methods

The fabrication of microencapsulated ammonium polyphosphate was seen in Figure 1. Encapsulated ammonium polyphosphate produced in accordance with the procedure described by Yang et. al., 2021. 200 g ammonium polyphosphate and 500 mL cyclohexane were loaded into a 1000 mL three necked reaction flask at 50 °C with stirring 1000 rpm for 20 minutes. After 25 g glycidyl methacrylate was transferred the reaction flask continued mixing for half an hour, then the temperature was increased to 80 °C. 0.4 g benzoyl peroxide was solved in 50 mL of butanone, and the resulting mixture was added to the reaction flask at this temperature and allowed to stir overnight. The resulting mixture was cooled to room temperature, washed with butanone, and dried in a vacuum oven at room temperature.

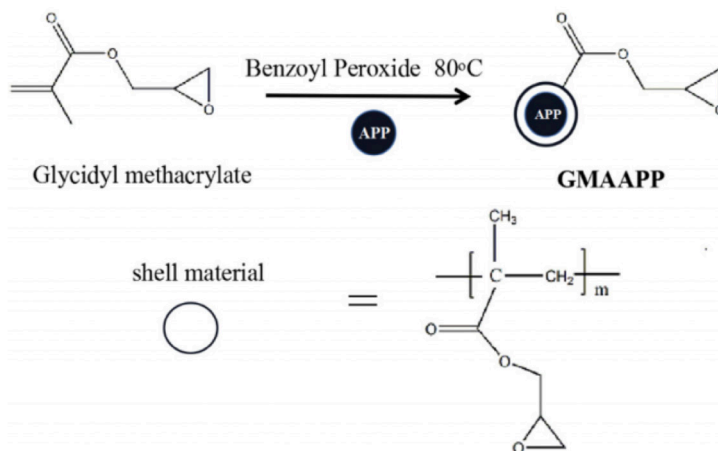


Fig 1. The encapsulation process of ammonium polyphosphate

100 g Polyether polyol (LY-4110), 1 g triethylenediamine, 2 g Silicone oil foam stabilizer and 3 g triethanolamine and 5 g distilled water and synthesized encapsulated ammonium polyphosphate were added into reaction flask. And the flask was stirred vigorously. After 150 g Polymethylene polyphenyl polyisocyanate was added to the mixture. The mixture was turned to White. The resulting precipitate was filtered. And then matured in an oven at 80 °C to complete the polymerization reaction.

The contents of the formulations prepared in order to provide flame retardancy properties to office type papers by using the obtained capsules are given in Table 1.

Table 1. Formulation of coatings

Sample	Starch (g)	Water (g)	Capsulated Ammonium polyphosphate (g)
F0	7.5	92.5	0
F1	7.5	92.5	1
F2	7.5	92.5	3
F3	7.5	92.5	5
F4	7.5	92.5	7.5

In the preparation of the coating formulation, a mixture of 7.5% starch and water was first prepared and mixed for about 15 minutes at 90 °C. The formulations were prepared by cooling the mixture to 55 °C and adding encapsulated ammonium polyphosphate at different rates. The obtained paper coating formulations were coated with a laboratory type K303 Multi-coater (RK Print Coat Instruments Ltd, United Kingdom) with using Mayer Rod 2, at room temperature onto amount of 0.1 g/m² to one side of 80 g/m² paper at a speed of 2 m/min. The average thickness of the coatings was set to 3 µm. The color, gloss contact angle-surface energies of the obtained coatings were determined by X-Rite eXact spectrophotometer and BYK Gardner glossmeter, PGX goniometer respectively.

Uncoated and enhcapsulated ammonium polyphosphate coated papers were printed with IGT C1 test printing machine using equal amounts of process magenta ink (DIN ISO 2846-1). Printing parameters; 300 N printing pressure and 0.2 m/s printing speed. The ink film thickness of all printed samples was measured as 8 µm. The color measurements of the prints on different coated paper were made by CIEL*a*b* method using X-Rite eXact spectrophotometer according to ISO 12647-2:2013 standard. The measure-

ment conditions of the spectrophotometer are determined as a polarization filter with 0°/45° geometry with 2 observer angles with D50 light source in the range of 400-700 nm. The difference between the colors of the different prints was calculated according to formula below according to the CIE ΔE 2000 ISO 13655 standard.

$$\Delta E_{00} = \sqrt{\left(\frac{\Delta L'}{k_L S_L}\right)^2 + \left(\frac{\Delta C'}{k_C S_C}\right)^2 + \left(\frac{\Delta H'}{k_H S_H}\right)^2} + R_T \frac{\Delta C'}{k_C S_C} \frac{\Delta H'}{k_H S_H} \quad (1)$$

The gloss measurements of coated papers were carried out with BYK Gardner GmbH micro gloss 75° geometry in accordance with ISO 82541:2009, and the gloss measurements of prints with BYK Gardner GmbH micro Tri-gloss 60° geometry in accordance with ISO 2813:2014.

The flammability characteristics of composites were determined by LOI. The LOI values of the coatings were measured by using a Fire Testing Technology (FTT) type instrument.

Results

In order to determine whether ammonium polyphosphate is encapsulated or not, the FTIR spectrum of both ammonium polyphosphate and encapsulated ammonium polyphosphate was examined and given in Figure 2. Ammonium polyphosphate is shown in black and the spectrum of encapsulated ammonium polyphosphate is shown in red. When the spectrum is examined, N-H stretching vibration can be clearly seen at 3200 cm^{-1} . In addition, P-O and P=O can be seen at 1100 cm^{-1} and 1250 cm^{-1} . Besides, the peaks at 1020 cm^{-1} and 805 cm^{-1} are PO₂ and P-O-P asymmetric stretching peaks, respectively. In the encapsulated ammonium polyphosphate, in addition to these peaks, the stretching peak of the C=O bond was observed at 1730 cm^{-1} , while the C=C at 1640 cm^{-1} disappeared. This shows that the encapsulation was successful. The results are consistent with the literature (Tang et al., 2014).

Figure 3 shows the SEM photograph showing the particle sizes of ammonium polyphosphate and microencapsulated ammonium polyphosphate. The particle sizes of ammonium polyphosphate and microencapsulated ammonium polyphosphate are around 10 μm . However, the surface of the clean and smooth ammonium polyphosphate became rougher by encapsulation. The results are in line with the literature (Chen et al., 2015).

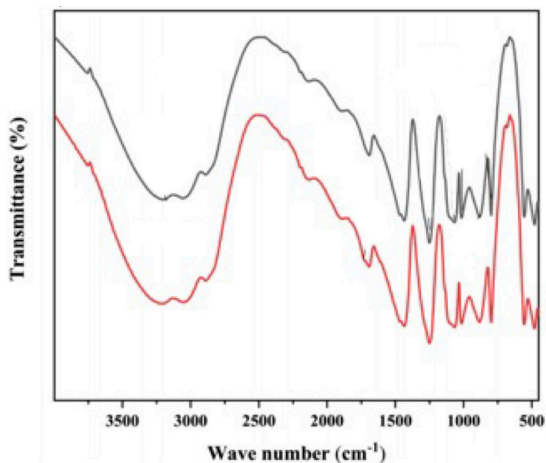


Fig 2. FTIR spectrum of ammonium polyphosphate and encapsulated ammonium polyphosphate

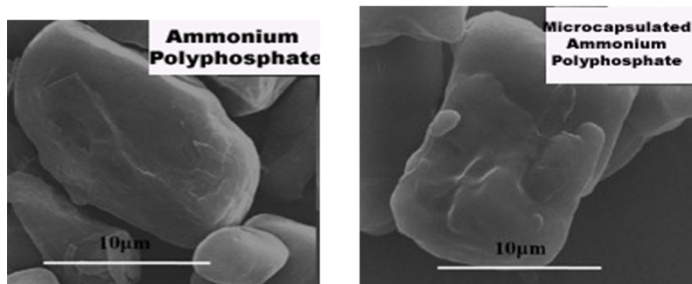


Fig 3. SEM images of ammonium polyphosphate and encapsulated ammonium polyphosphate

Coatings containing encapsulated ammonium polyphosphate were prepared in the compositions in Table 1 and coated on the paper surface without any problems. The thicknesses of the resulting coatings were set to 3 μm . One of the main parameters for printing on the obtained papers is the establishment of the relationship between the ink and the substrate without any problems. This is a relationship that depends on the surface energy and the contact angle. In this sense, the contact angles and surface energies of the papers were measured and given in Table 2 in order to be able to print without problems. When Table 2 was examined, it was determined that the

contact angles of all coatings containing encapsulated ammonium polyphosphate were lower than the coating containing only starch. When the literature is examined, it has been observed that the contact angle of the coatings containing ammonium polyphosphate decreased due to the -NH₄ contact angle groups on the ammonium polyphosphate, and the contact angle of all coatings to which the ammonium polyphosphate was added decreased up to 10° (Zheng et al., 2014a). For this reason, the materials become weakly resistant to water and moisture. For this purpose, it was aimed to use encapsulated ammonium polyphosphate in our study. As seen in Table 2, the contact angle decreased in coatings containing encapsulated Ammonium polyphosphate. However, it appears to have considerably higher water resistance and contact angle than this unencapsulated ammonium polyphosphate. As the amount of flame retardant material in the coating increases, the contact angle decreases more. In short, coatings to which ammonium polyphosphate added can be better printed with water-based inks and are water-labile, while coatings containing encapsulated polyphosphate have been made water-resistant and more suitable for oil-based ink. The results are consistent with the literature (Zheng et al., 2014b).

Table 2. Contact angle and surface energies of coatings

Sample	Contact Angle (°)	Surface Energy (mJ/m ²)
F0	72.3	38.9
F1	51.0	42.7
F2	49.6	45.9
F3	40.0	52.7
F4	35.5	58.4

The flame retardancy properties of microencapsulated ammonium polyphosphate content paper coatings were examined with LOI measurements. LOI is a widely used technique to determine the flame retardancy of coatings. LOI values of the coated papers are given in Figure 4. When the figure is examined, the flame retardancy feature is increased by adding encapsulated ammonium polyphosphate into the F0 coating, which shows extremely flammable properties. As the amount of encapsulated ammonium polyphosphate in the content increased, the fire resistance increased and reached approximately double in the coating containing 10%. Ammonium polyphosphate gives the composite material a flame retardant property with the formation of ash, which causes a decrease in mass and heat transfer be-

tween the solid phase and the burning surface. Similar results can be seen in the literature (Savaş and Doğan, 2018).

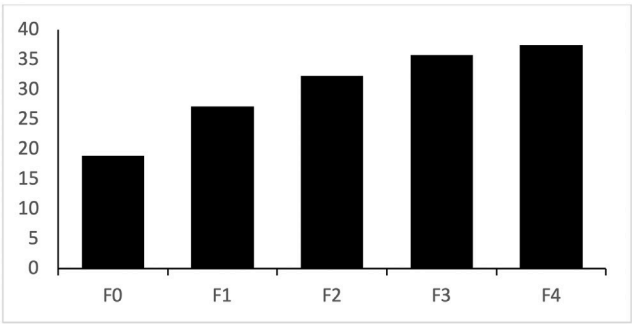


Fig 4. LOI values of coated papers

Table 3 shows the CIEL*a*b* color, gloss and color differences of the encapsulated ammonium polyphosphate coated paper. Untreated base paper was used as reference. When the color differences were examined, it was determined that the F0 starch coated paper color shifted slightly to yellow compared to the base paper. This is an expected result (Wang et al., 2021). It was determined that when encapsulated ammonium polyphosphate was added to the coating formulations, the color shifted to a small amount of blue. This is due to the color of the added ammonium polyphosphate and is an expected result. The color change (ΔE) is in the range about 0.44-1.35. It is also within the acceptable reference range according to ISO 12647-2:2013. When the gloss values were examined, it was determined that all coatings were at least 4.5 times glossier than the base paper. This is due to the fact that the roughness on the paper surface is covered by the coating and the diffuse reflection is prevented. Thus, the papers became glossier. The results are similar to the literature (Chinga and Helle, 2003).

Table 3. Color and gloss values of flame retardant paper coatings

Sample	L*	a*	b*	ΔE_{00}	Gloss
F0	95.46	2.91	-10.21	Standard	5.7
F1	95.31	2.87	-8.45	1.27	28.2
F2	95.28	3.02	-10.84	0.44	27.5
F3	94.93	3.17	-11.34	0.85	27.2
F4	94.41	3.49	-11.82	1.35	26.9

Offset test prints were made on coated papers containing encapsulated ammonium polyphosphate in different ratios, and color and gloss characters were examined and given in Table 4. When the color character is examined in Table 4, it is determined that the results are parallel to the non-printed papers. In other words, it was determined that the coating containing starch slightly shifted the color of the paper to yellow, while the coatings containing encapsulated ammonium polyphosphate slightly shifted the color to blue. The results obtained are compatible with the literature (Ozcan et al., 2020). Since the ΔE differences in the unprinted papers are tolerated by the magenta ink in printing, the color difference has decreased in the prints. The color differences of the prints on all coatings are within the tolerance limits according to ISO 12647-2. When the gloss values were examined, parallel results were obtained. The reason for the decrease in gloss of all prints is that the pigment in the ink distributes the light slightly. Thus, surface roughness and diffuse reflection increased, gloss decreased.

Table 4. Color and gloss values of printed papers

Sample	L*	a*	b*	ΔE_{00}	Gloss
F0	47.24	73.94	-3.55	Standard	1.9
F1	47.09	73.86	-1.63	0.92	19.8
F2	46.87	74.05	-3.94	0.42	17.6
F3	46.75	74.21	-3.47	0.50	17.2
F4	46.38	74.59	-3.95	0.82	16.6

Conclusions

In this study, ammonium polyphosphate was encapsulated to make flame retardant coatings more resistant to water. It has been proven by FTIR that the capsules were successfully synthesized, and the size of the capsules obtained was measured by SEM at 10 μm . Starch-based coating formulations were prepared with the obtained capsules and successfully coated on the office paper surface. The contact angle and surface energy of the coatings were measured. The contact angle of ammonium polyphosphate in the literature has been increased by encapsulation, so that the coated papers produced can be printed with oil-based offset ink. When the LOI properties of the coatings containing encapsulated ammonium polyphosphate in the coatings were examined, it was determined that the paper gained flame retardancy property and the property increased with the increasing ammonium polyphosphate ratio. When the color properties of the coated papers were examined, it

was measured that the color difference decreased even more with the prints where the color shifted to blue very little. It was determined that the surface became smooth and the gloss increased with the coatings made. As a result, papers that can be printed with oil-based ink with high flame retardancy properties have been successfully produced with encapsulated ammonium polyphosphate.

References

1. Bee, S. T., Lim, K. S., Sin, L. T., Ratnam, C. T., Bee, S. L., & Rahmat, A. R. (2018). *Interactive effect of ammonium polyphosphate and montmorillonite on enhancing flame retardancy of polycarbonate/acrylonitrile butadiene styrene composites*. Iranian Polymer Journal, 27(11), 899-911.
2. Chen, M., Tang, M., Qi, F., Chen, X., & He, W. (2015). *Microencapsulated ammonium polyphosphate and its application in the flame retardant polypropylene composites*. Journal of Fire Sciences, 33(5), 374-389.
3. Chinga, G., & Helle, T. (2003). *Relationships between the coating surface structural variation and print quality*. Journal of pulp and paper science, 29(6), 179-184.
4. Kandirmaz, E. A., Ozcan, A., & Ulusoy, D. E. (2020). *Production of thermochromic microcapsulated inks for smart packaging and examination of printability properties*. Pigment & Resin Technology. 49(4), 273-281.
5. Li, M., & Wu, Z. (2012). A review of intercalation composite phase change material: preparation, structure and properties. Renewable and Sustainable energy reviews, 16(4), 2094-2101.
6. Ozcan, A., Kasikovic, N., Arman Kandirmaz, E., Durdevic, S. and Petrovic, S. (2020). *Highly flame retardant photocured paper coatings and printability behavior*. Polymers for Advanced Technologies, 31(11), 2647-2658.
7. Qu, H., Wu, W., Hao, J., Wang, C. and Xu, J. (2014). *Inorganic-organic hybrid coating-encapsulated ammonium polyphosphate and its flame retardancy and water resistance in epoxy resin*. Fire and materials, 38(3), 312-322.
8. Rezvani Ghomi, E., Khosravi, F., Mossayebi, Z., Saedi Ardahaei, A., Morshedi Dehaghi, F., Khorasani, M., Neisiany, R.E., Das, O., Marani, A., Mensah, R.A. and Jiang, L. (2020). *The flame retardancy of polyethylene composites: From fundamental concepts to nanocomposites*. Molecules, 25(21), 5157.
9. Savaş, L.A. and Doğan, M. (2018). *The role of expandable graphite and organoclay on the flame retardant and mechanical properties of carbon*

- fiber filled intumescent polypropylene composites*. Journal of Textiles and Engineer, 25(109), 22-29.
10. Tang, Q., Wang, B., Tang, G., Shi, Y., Qian, X., Yu, B., Song, L. and Hu, Y. (2014). *Preparation of microcapsulated ammonium polyphosphate, pentaerythritol with glycidyl methacrylate, butyl methacrylate and their synergistic flame-retardancy for ethylene vinyl acetate copolymer*. Polymers for advanced technologies, 25(1), 73-82.
 11. Venkatram, M., Narasimha Murthy, H.N.R., Gaikwad, A., Mankunipoyil, S.A., Ramakrishna, S. and Ayalasomayajula Ratna, P. (2018). *Anti-bacterial and flame retardant properties of Ag-MgO/nylon 6 electrospun nanofibers for protective applications*. Clothing and Textiles Research Journal, 36(4), 296-309.
 12. Wang, B., Sui, J., Yu, B., Yuan, C., Guo, L., Abd El-Aty, A.M. and Cui, B. (2021). *Physicochemical properties and antibacterial activity of corn starch-based films incorporated with Zanthoxylum bungeanum essential oil*. Carbohydrate Polymers, 254, 117314.
 13. Xia, Y., Liu, S., Wang, X., Han, Y., Li, J. and Jian, X. (2008). *The analysis of synergistic effects of zeolites applied in intumescent halogen-free flame-retardant ABS composites*. Polymer-Plastics Technology and Engineering, 47(6), 613-618.
 14. Xie, F., Wang, Y.Z., Yang, B. and Liu, Y. (2006). *A novel intumescent flame-retardant polyethylene system*. Macromolecular Materials and Engineering, 291(3), 247-253.
 15. Yang, Y., Dai, Z., Liu, M., Jiang, H., Fan, C., Wang, B., ... & Wang, H. (2021). *Flame retardant rigid polyurethane foam composites based on microencapsulated ammonium polyphosphate and microencapsulated expanded graphite*. Journal of Macromolecular Science, Part A, 1-10.
 16. Zheng, Z., Qiang, L., Yang, T., Wang, B., Cui, X. and Wang, H. (2014a). *Preparation of microencapsulated ammonium polyphosphate with carbon source-and blowing agent-containing shell and its flame retardance in polypropylene*. Journal of Polymer Research, 21(5), 1-15.
 17. Zheng, Z., Sun, H., Li, W., Zhong, S., Yan, J., Cui, X. and Wang, H. (2014b). *Co-microencapsulation of ammonium polyphosphate and aluminum hydroxide in halogen-free and intumescent flame retarding polypropylene*. Polymer composites, 35(4), 715-729.

ИССЛЕДОВАНИЕ КАЧЕСТВА ОТТИСКОВ ТЕРМОТРАНСФЕРНОЙ ПЕЧАТИ НА РАЗЛИЧНЫХ ТКАНЯХ

Назар О. Р.

Украинская академия печати

Abstract

Experimental studies of the quality of printed images by thermal transfer printing on fabrics of various compositions, in particular polyester (100%); cotton (100%) and fabric composition (60% polyester and 40% cotton) have been done. Transfer printing is performed on TD 380 TH press of the company Everbright Machinery Co. LTD at technological modes (temperature 140 – 160 °C, time 5-15 s, pressure 3-4 Bar). The quality of the line reproduction in the system: photoplate – stencil plate – decal (transfer) – imprint on fabric is studied. The synthetic paper from Hicotex company is used for the decal manufacturing. The ink fixing on the imprint takes 3 minutes using a Mikon flash dryer. A model test-form is used to assess the quality, on which a scale for the optical density assessment, a text, and a scale for the excretory capacity assessment are applied. The line thickness is determined using MPB-2 microscope, and the optical density is measured with Gretag SPM 50 densitometer. The studies have shown that the graphic line distortions are observed in the process of transferring small elements on the fabrics under study. Significantly higher quality of lines is observed on 100% polyester fabric. This may be due to the fabric texture and the varying degrees of ink absorption. As a result of the research, graphical dependencies have been constructed, which make it possible to assess the quality of thermal transfer printing and the accuracy of image reproduction on various fabrics.

Keywords: *thermal transfer printing, synthetic fabric, quality, optical density, plastisol inks.*

Постановка проблемы

Термотрансферная печать – уникальная технология, позволяющая запечатывать различные материалы. На современном этапе такой способ печати пользуется большой популярностью и многие компании интересуются этим рынком. Объясняется такой спрос скоростью выполнения

заказов, возможность печатания небольших тиражей по приемлемой цене, широкий ассортимент материалов для запечатывания, высокое качество печати – основные преимущества термотрансферной печати. Используя не прямые способы трафаретной печати, современные полиграфические предприятия имеют возможность изготавливать широкий ассортимент не издательской продукции высокого качества. Доля использования термотрансферной печати в последние годы заметно увеличивается.

Термотрансферная печать – один из не прямых способов трафаретной печати, который отличается простотой и доступностью изготовления печатных форм. Печать может с успехом осуществляется на разнообразных материалах и готовых изделиях в условиях практически любого полиграфического производства, не требуя больших затрат. Кроме того, предоставляется широкая возможность работать с материалами большого формата, использовать новые материалы, например, краски и лаки для достижения различных спецэффектов.

Главная задача термотрансферной печати – получение оттисков заданной толщины красочного слоя, а также обеспечить необходимую градационную точность изображения. Технология этого способа печати, к сожалению, не позволяет точно прогнозировать графические и градационные искажения. Поэтому проведение исследований характеристик оттисков термотрасферной печати на тканях является сегодня актуальной задачей.

Цель статьи – оценка качества оттисков термотрансферной печати на различных тканях.

Объекты и методы исследования. Объекты исследования – оттиски на различных тканях, а именно: 100% полиэстер; 60% полиэстер и 40% хлопок и 100% хлопок.

Методика исследования

Для оценки качества использовали модельную тест-форму, на которой были нанесены шкала для оценки оптической плотности, текст, шкалы для оценки выделяющей способности.

Вывод фотоформ проводили на фотовыводном устройстве Dolev 4 press фирмы Scitex. Копировальный слой наносили на сита-основы с тремя видами ситовой ткани: № 100.40 (имеет плотность 100 нит/см и соткана из полиэфирной нити диаметром 40 мкм); 120.34 (имеет плотность 120 нит/см и соткана из полиэфирной нити диаметром 34 мкм); 140.34 (имеет плотность 140 нит/см и соткана из полиэфирной нити диаметром 40 мкм); Копировальный слой наносился вручную при помощи

ракеля-кюветы Agabe шириной 37 см, с обеих сторон сетки. Использовался копировальный раствор Dirasol 916 фирмы Fuji Film. Время высыхания эмульсии 30–40 мин. Экспонирование фотоформ проводили в копировальной раме фирмы Bestel оснащенной УФ-лампой мощностью 3500 Вт. Проявление печатных форм водой проводили в ванной для проявки Karcher K5 Compact на протяжении 1–15 с. Для высушивания печатных форм использовали сушильный шкаф EB 1300 HX HX-Tech. Время высушивания 20–25 мин.

В качестве материала для деколей использовали синтетическую бумагу фирмы Nicotex. Печать деколей проводили на ручном трафаретной машине карусельного типа фирмы Anatol. При печати использовали пластизольные краски серии NF триадный комплект: NF 82 (Magenta), NF 83 (Yellow), NF 84 (Cyan), NF 85 (Black) фирмы Antex. Краски наносили ракелем фирмы Sebilob твердостью 75 ед. по Шору. Закрепления красок на оттиске проходило в течении 3 с использованием флеш-сушки фирмы Mikon. Для закрепления краски на деколях использовали туннельную сушку Mikon Sir+A. После чего на деколи наносили порошковый крупнодисперсный трансферный клей TM 2000 для лучшей адгезии к ткани. Оттиски сушили с помощью туннельной сушки Mikon Sir+A.

Трансфер на различные виды ткани (1–100% полиэстр; 2–60% полиэстр и 40% хлопок; 3–100% хлопок) переводили на прессе TD 380 TH фирмы Everbright Machinery Co. LTD на протяжении 5–15 в производственных условиях. По каждому показателю за окончательный результат принято среднее значение нескольких измерений минимум по трем оттискам. Толщину штрихов определяли с помощью микроскопа МПБ-2, а, оптическую плотность измеряли денситометром Gretag SPM 50.

Результаты исследований. Результаты воспроизведения штрихов на тканях приведены в табл. 1.

Из табл. 1–3 видно, что штрихи воспроизведены с некоторыми отклонениями по ширине. Анализ оттисков показывает, что края у штрихов, полученных с формы на ситовой ткани № 140, являются более четкими. Это объясняется тем, что сама сетка тоньше, по сравнению с сетками 100 и 120.

Характерной особенностью процесса является то, что вначале изготавливают деколь, т.е. изображение печатают трафаретным способом на промежуточной основе (синтетической бумаге), затем переносят на готовое изделие или полуфабрикат под действием высокой температуры и давления.

Таблица 1. Графические искажения штрихов, отпечатанных с ситовой ткани № 100 на исследуемых тканевых образцах (1 – 100% полиэстер; 2 – 60% полиэстер и 40% хлопок; 3 – 100% хлопок)

Ширина штриха на фотоформе, мм	Ширина штриха на образце № 1	Ширина штриха на образце № 2	Ширина штриха на образце № 3
0,1	0,13	0,11	0,11
0,2	0,15	0,15	0,14
0,3	0,16	0,16	0,15
0,4	0,19	0,21	0,17
0,5	0,24	0,22	0,22

Таблица 2. Графические искажения штрихов, отпечатанных с ситовой ткани № 120 на исследуемых тканевых образцах (1 – 100% полиэстер; 2 – 60% полиэстер и 40% хлопок; 3 – 100% хлопок)

Ширина штриха на фотоформе, мм	Ширина штриха на образце № 1	Ширина штриха на образце № 2	Ширина штриха на образце № 3
0,1	0,12	0,10	0,09
0,2	0,11	0,12	0,12
0,3	0,14	0,13	0,14
0,4	0,16	0,19	0,16
0,5	0,21	0,21	0,19

Таблица 3. Графические искажения штрихов, отпечатанных с ситовой ткани № 140 на исследуемых тканевых образцах (1 – 100% полиэстер; 2 – 60% полиэстер и 40% хлопок; 3 – 100% хлопок)

Ширина штриха на фотоформе, мм	Ширина штриха на образце № 1	Ширина штриха на образце № 2	Ширина штриха на образце № 3
0,1	0,10	0,08	0,07
0,2	0,10	0,10	0,10
0,3	0,12	0,11	0,12
0,4	0,14	0,14	0,15
0,5	0,20	0,20	0,18

Кроме того, деколь, как правило, снимают сразу после открытия пресса, когда краска все еще горячая, в результате чего пленка краски разделяется между бумагой и тканью.

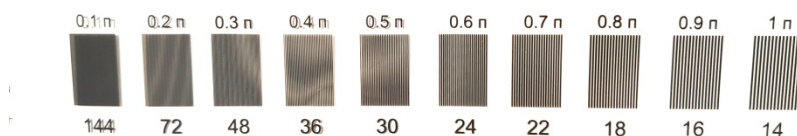


Рис. 1. Тестовая фотоформа для исследования термотрансферной печати

Анализируя изображения штрихов шкалы выделяющей способности (рис. 1), можно сделать вывод, что в процессе переноса мелкие элементы воспроизведены с незначительными искажениями. Что касается элементов 0,5 п.; 0,6 п. и 0,7 п., то они воспроизведены на образцах тканей 100 % хлопок; б – 60 % полиэстер и 40 % хлопок со значительными отклонениями. Лучшие результаты показывает образец 3 (ткань 100 % полиэстер). Возможно, это связано со структурой ткани и с различной степенью поглощения краски.

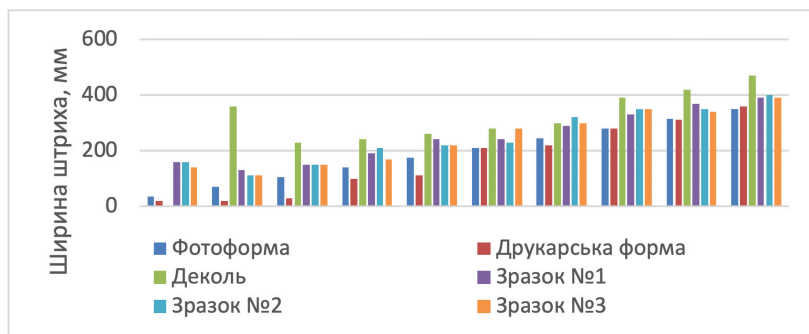


Рис.2. Ширины штрихов выделяющей способности на образцах:
1 – 100 % полиэстер; 2 – 60 % полиэстер и 40 % хлопок; 3 – 100 % хлопок
при линейтуре 100 нит./см

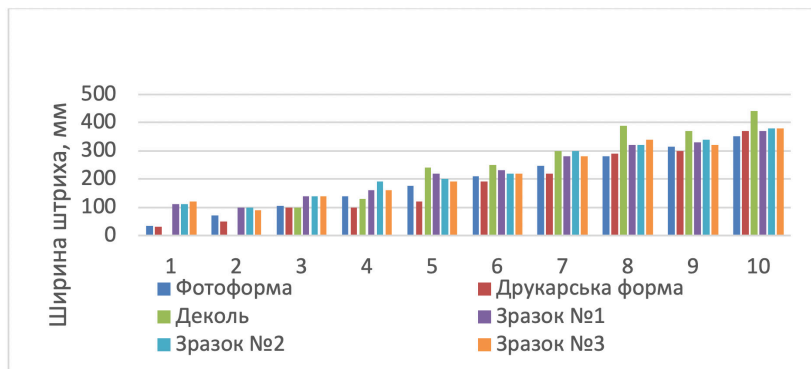


Рис.3. Ширины штрихов выделяющей способности на образцах: 1 – 100% полиэстер; 2 – 60% полиэстер и 40% хлопок; 3 – 100% хлопок при линиатуре 120 нит./см

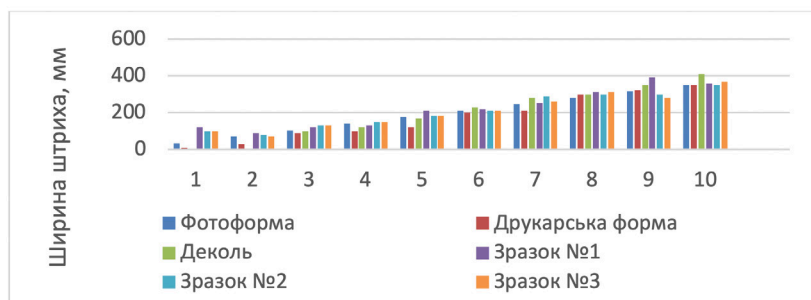


Рис. 4. Ширины штрихов выделяющей способности на образцах: 1 – 100% полиэстер; 2 – 60% полиэстер и 40% хлопок; 3 – 100% хлопок при линиатуре 140 нит./см

Выводы

Наилучшие показатели качества получены на ткани 100% полиэстер, что связано с гладкой и ровной структурой ткани. Результаты денситометрических показателей для тканей 100% хлопок и 60% полиэстер и 40% хлопок показывают невысокие результаты, особенно для образца 3, воспроизведенного при линиатуре ситовой ткани 140 нит./см. Это можно объяснить микронеровностями поверхностей этих тканей.

Список литературы

1. S. Havenko, N. Menżyńska, S. Khadzynova. Ocena jakości nadruku termotransferowego na etykietach i metkach odzieżowych / S. Havenko, // Przegląd paperniczy. – 2013. – № 9. – S. 481- 485.
2. Ткаченко В. П. Оперативні та спеціальні види друку. Технологія, обладнання: навч. посібн. - В. П. Ткаченко. – Харків, 2005. – 335 с.
3. Тканина бавовна. [Електронний ресурс]. – Режим доступу: <https://rukodeli.com.ua/tkanina-bavovna-povnii-opis/>.

THE EFFECT OF DIGITALIZATION ON ILLUSTRATION IN GRAPHIC DESIGN

Ozcan A., Cidik E., Kandirmaz E.A.

Marmara University, School of Applied Sciences

Abstract

Illustrations that support the visual aspect of the graphic arts are visual images used to interpret, depict, explain or embellish content in books, newspapers and online media. The communication process, which evolved from the drawings on the cave walls to writing, is insufficient on its own. Illustrations can express a feeling, a meaning or an essence more effectively than a wall text can. Illustrations can simplify a complex idea, complement the words or message expressed to the user, and can sometimes stand alone without any necessary explanation. Illustrations continue to take a permanent place in our lives by enabling us to give details that cannot be seen in photography or to express imaginary ideas or thoughts with digitalization. Today, with wider and more efficient distribution networks, illustrated newspapers, books and magazines find a suitable distribution area. Both graphic design and illustration have their own techniques and tools. With digitalization, these tools are developing and reaching a level that every user can achieve. With different types of software, illustrators develop their own artistic forms. The illustrations, which were previously made with computers, have now been replaced by graphic drawing tablets.

In this study, it is aimed to draw attention to the illustrations that help the sector trying to keep up with the digitalized world, to research the techniques used and new technology products. For this purpose, the types of illustration were researched, the traditional techniques still used today and the developing digital tools were examined. The developments experienced with digitalization in illustrations, the effects of produced software and applications on graphic design are discussed.

Keywords: *Illustration, Digitalization, Graphic design, Graphic tablet*

Introduction

Illustration and Graphic Design

In terminology, illustration is defined as a picture that is functional to explain something. Etymologically, the word “illustration” comes from the Latin word “Illustrate”, which means explanation. It is also said that illustrations are derived from the word illusion. This occurs as a complement to a goal to help a person more easily understand the message in a picture. Illustration, which is a two-dimensional work of art, is used to clarify an understanding. Illustrative pictures are used to decorate books, magazines or newspapers in certain columns. Illustration is usually a form of visual text or sentence. For those who love illustration, besides being interesting with its unique and various messages, it is an educational opportunity for children who are more interested in painting as they cannot read well. Illustrations can also describe scenes in a story, so illustration usually describes the character or the entire story content (Zeegen 2009; Özcan et al. 2018).

Historically, book illustration and magazine/newspaper illustrations have been the dominant forms of such visual arts, but illustrators have also used their graphic skills in poster art, advertisements, comics, animation art, greeting cards, and cartoon strips. Most illustrative illustrations are made with pen and ink or metal nib, then reproduced using a variety of printing processes, including lithography, photography, and engraving (Liu 2021).

Graphic design is an art, professional and academic discipline that consists of reflecting visual communication that aims to convey specific messages to social groups with specific goals. Therefore, it is an interdisciplinary branch of design whose basis are defining problems and setting goals for decision making, creativity, innovation and lateral thinking, as well as digital tools that transform them for correct interpretation. This activity helps in optimizing graphic communication. The role of the graphic designer in the communication process is the encoder or interpreter of the message (Chu 2018). They work on the interpretation, organization and presentation of visual messages. Design work always starts from a client's request, a linguistically manifested request, verbally or in writing, that is, graphic design transforms a linguistic message into a graphic representation. Graphic design, as a field of application, has different fields of knowledge that focus on any visual communication system (Ambrose, Harris & Ball 2019).

Illustration Types

Illustrations make a deep and long-term impact on the human mind. When used appropriately, they become a powerful mechanism for rich storytelling and marketing. Illustration, one of the most widely used tools of visual com-

munication, has been developing over the years to gain a strong identity in the publishing, packaging, healthcare, education and production industries. Illustrations can be integrated into books, learning materials, animations, posters, flyers, magazines, movies and indeed all kinds of print and digital media. Any idea or concept can be presented in a more interesting way using illustration. With the developments in technology and the increasing importance of illustration for some different fields, it has brought brand new styles to illustration techniques. With the developing technology and the tools used, new products are emerging (Klimowski 2012).

With digitalization, illustrations have started to be used frequently in the film and advertising industry, and in a number of other areas. The expensiveness of advertising and film productions or the difficulty of movie shooting due to the pandemic we live in today have pushed artists to use illustrations. The fact that illustrations can be applied to both traditional methods and digital methods is an advantage for artists.

Advertising Illustrations

Advertising illustrations are graphic images that clarify texts, direct the eyes of the target audience and create a lasting impression. Illustrations are included in ad layouts to convey one or two concepts to viewers. The purpose of advertising illustrations is to enhance the message of the accompanying text and to attract the consumer to read the text. Illustrations persuade potential customers to buy the product and maintain awareness (Figure 1).



Fig 1. J.C Leyendecker's 1915 Kellogg's advertising illustration

Advertising illustrations appear in almost every part of our lives. According to other application areas, there are many different uses such as billboards, television advertisements, flyers, posters, direct mail kits, web banners, bus stops.

Scientific Illustrations

Scientific illustrations are drawings that have a scientific subject or purpose aimed at conveying information. Today, sculpture, ink, watercolor, colored pencil, digital illustration and animation are widely used tools in science illustration (Wood 1994). Scientific illustrations are used in textbooks, brochures, magazines, user manuals, scientific publications, and botanical gardens (Figure 2).



Fig 2. A *Magnolia* species coloured etching by G. D. Ehret (<https://www.botanica-lartandartists.com/about-georg-ehret.html>)

Technical Illustrations

Technical illustration is a field of drawing that uses static and dynamic images to explain the interconnectedness of technical operations. Technical illustrations detail a complex mechanism or product by making it visually simple. It aims to create effective images that effectively convey certain information to the observer through the visual channel. It generally continues its activities in broadcast media, medicine, engineering and scientific fields. Illustrators working in the technical field make technical and electronic manuals and assembly instructions available to people through this branch (Figure 3).



Fig 3. Technical illustration, Rescue Helicopter Section for United Technologies campaign – Hans Jenssen (<https://www.hansjenssen.co.uk/cross-sections>)

Children’s Book Illustrations

Children’s book illustrations include all kinds of pictures produced especially for books aimed at young audiences. In particular, illustrations are needed in stories to improve children’s communication skills and expression potential. Illustrations in children’s books draw attention visually and offer children a fun narrative structure. With these visual representations, their imagination gets rid of a limited expression (Figure 4).



Fig 4. İrem Ustaoglu, “Monster Puh and Brave Suzi”, Children’s book Illustration work (<https://www.behance.net/gallery/114928483/Monster-Puh-and-Brave-Suzi-%28thaki%29>)

Infographics

Infographics are visual representations of information or data. It consists of an image, chart, and minimal text that provides an easy-to-understand overview of a topic. In infographics, striking and interesting visuals are used to convey information quickly and clearly. Therefore, they are valuable tools for visual communication. Marketers prefer infographics to create brand awareness and increase interaction. The purpose of infographics is not only to inform, but also to present entertaining and interesting content to the target audience (Figure 5).

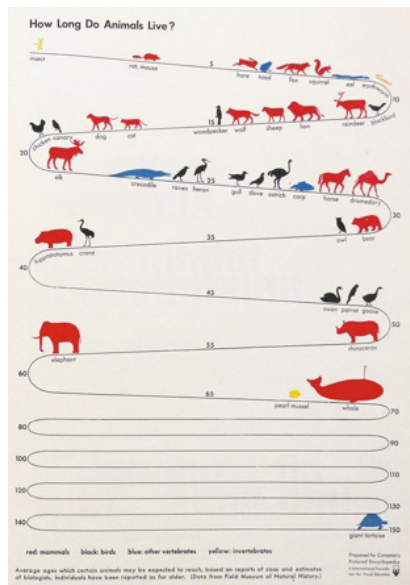


Fig 5. Gerd Arntz, Infographic Showing the Habitat of Animals (<https://datavizblog.com/2013/08/06/dataviz-history-isotype-charts-the-vintage-visual-language-that-gave-rise-to-modern-infographics/>)

Archaeological Illustration

Archaeologists use illustrations to describe artifacts from the remains. Today, archaeologists prefer computer and graphic software to produce illustrations. The purpose of archaeological illustrations is to provide more information in a format that the audience can read (Figure 6). They figure works for interpretation on websites, books, and research papers. By displaying an archaeological illustration of a finding, an accurately sized draw-

ing is obtained showing the details of the object's decoration, type, form, and even construction method. Archaeological illustrations are usually black and white. The main purpose is to reveal the decoration and show the depth of the object. Colors are rarely added to academic pictures. It is only added to highlight details such as glazes or colors in painted glass.

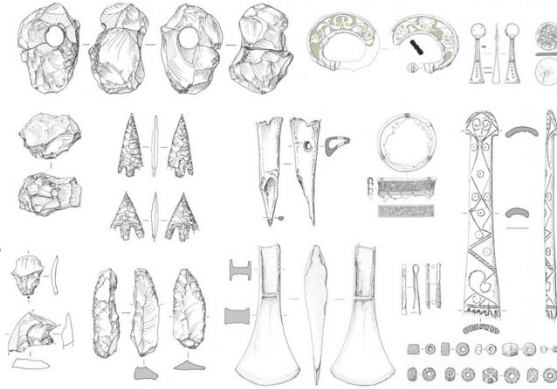


Fig 6. Illustration sample from *Artifacts from Archaeological Studies* (<https://www.wessexarch.co.uk/archaeological-services/artefact-publication-illustration>)

Illustration in the Digital World and Digital Methods Used in Illustration

The illustrations were used by upper-class nobility before the 1500s, representing the cultural identity of the church. In the Renaissance period, the art of illustration became a desirable and valued art and spread to the world as a visual culture. Digital illustration, on the other hand, took its first steps for development shortly after World War II. In the 1960s, when scientific research on computation and algorithms was carried out, it gained great momentum. Creative experiences created with the help of computers in the period between 1950 and 1970 have been a period of innovation for today's illustration art and animation industry. After studies, the ability to program computers to perform specific tasks and the improvement of imaging systems allowed illustrators or artists to input directly. In this way, it is possible to manipulate the images pixel by pixel in order to achieve the desired goal. Thus, the foundations of digital painting and drawing were laid. Between the 1970s and 1990s, illustrators and artists began to see how technology could be used to transform existing images into new works with the available possibilities. Most of these artworks are basically created from

vector images different from pixel images. Unlike pixel images, vector images can be dimensioned endlessly without losing resolution. Developments between 1980 and 1990 began to encompass both the viewer and the artist, interactive environments placed at the interface between the real and virtual worlds. Illustrators are focused on manipulating images with the help of computer software tools. In this way, in the digitalized world, art has become easy to reach and visible for every class and every person. Illustrators can make their works visible to millions of people from all over the world at great speed by uploading them online thanks to the internet (Husarik 2007).

The major developments in the 21st century we live in are changing the way we communicate, our lifestyle and the way we watch movies, which have evolved into the digital world, at the same speed. As the world digitizes, the data obtained through concrete and natural means is reset. Despite this, the illustrations continue on their way by transforming. An area is emerging where technology and illustration combine to create a new natural identity. With the use of computer aided design in the new digital world created, concepts such as new media art have become more audible today. New media art is a term that covers art forms that are produced, modified and transmitted through digital technologies. It is a branch that can be used generally connected to the internet and provides interaction with users. With the social and cultural changes in the society, it has created a space for new contemporary art practices. In new media art, artists often collaborate because of the need for a wide variety of artistic skills to be executed. The use of various graphic tablets and social media has also increased the number of illustrators. Artists and illustrators who want to increase their followers on social media have been in search of new ideas (Meyer, Schaupp & Seibt 2019).

Digital Methods Used in Illustration

There are many forms of digital approaches found in different infrastructures used in illustrations or artistic drawings. Today, as the materials and digital illustration tools used change and develop, different techniques and approaches emerge. Different tools can be used according to the wishes of the artists in order to obtain the desired image quality or to manipulate the images easily.

Vector Based Illustration

Vector illustration is an art formed of vector graphics. It is created using vector drawing software programs such as Adobe Illustrator. These charts are based on mathematical formulas. Illustrations are usually composed of points, lines and curves as the main structure. When vector illustrations are

rescaled according to the variety of work, their resolution and image quality are not lost.

Due to its ability to integrate with Adobe Photoshop, it is an ideal method for processing poster-style works by exchanging photos. Works made using vector software such as Adobe Illustrator are considered vector illustrations. The use of vectors has become widespread due to the laboriousness of creating raster images and the expensive computational power required. All of the text vectors used today are made in vector-based programs.

Pixel Based Illustration

Pixel-based illustrations consist of small colored or colorless squares that can be seen when zoomed in and form the whole image. Their image quality is lower compared to vector-based illustrations. Pixel-based illustrations may experience problems with rescaling. Especially when the image is zoomed in, breaks occur in the edge lines. In illustrations created using this method, it is possible to make smoother transitions between colors by increasing or decreasing the color of pixels or shadows. Thus, smoother color mixtures can be obtained. It is possible to animate illustrations with various brushes and effects included in software such as Adobe Photoshop or Procreate. Unlike vector-based illustrations, smooth color transitions can be achieved with the help of brushes instead of clear and sharp transitions.

Pixel art is a form of digital art in which images or photographs are created or edited at the pixel level using graphics editing software. Pixel Art is created from large visible pixels that make up the constituent elements of the entire image.

Today, vector graphics have taken the usage areas of Pixel Art. Illustrators and artists use Pixel Art as an artistic choice. While a simple program such as Microsoft Paint can be used, a more comprehensive program such as Adobe Photoshop can also be used. In the game industry, although 3D software dominates the market, pixel art still exists.

Photo Manipulation

Photo manipulation is the process of transforming the image by using various methods and techniques to achieve the desired results in photography. Photo manipulation may also be used in science fiction elements. However, in the images created, surreal scenes should still have realistic perspective, lighting and shading (Wilson 2016). In order to achieve the required level of realism, photographs that are independent of each other, but also complement each other, should be combined. Generally, Adobe Photoshop software is used, where the image can be processed best.

Animated Illustration

GIF is a commonly used image file format for images on websites and motion graphics in software programs. Illustrations saved in this format offer lossless compression without reducing the quality of the image. GIF images can contain a maximum of 256 colors. They are also loops where the first and last frames are exactly the same. With such illustrations, it is possible to achieve the desired results in storytelling or explaining the subject. Animated illustrations are gaining popularity today as they convey jokes, emotions and ideas. The use of animated illustrations in integration with applications such as Twitter, Facebook and Instagram have become widespread.

Illustration Tools Emerged with Digitization

Digital illustration is the process of creating images and works using digital tools. It is made with Adobe Illustrator, Photoshop and similar applications. In addition, it is used in tools such as computers, mouse, stylus pen, drawing tablets. Many of these tools are inspired by the materials used in traditional illustration. With these tools that have become widespread, a more flexible and comfortable working area has been created in illustration. Therefore, the demand for these vehicles is increasing rapidly today. Likewise, with the increasing demand, the vehicles used are renewing themselves and new types of vehicles are emerging.

Computer

Illustrators and artists first experimented with computers in the 1950s. By the 1970s, the light pen or stylus pen was introduced to the market. In this way, users started to move items freely on the computer monitor. Today, stylus type pens are still in the foreground compared to the mouse. The advent of the inkjet printer in 1976 facilitated the printability of works of art.

After the 1990s, illustrators focused on manipulating images with the help of computer software. Thus, companies such as Adobe have produced vector or pixel-based software programs that appeal to users. The digital manipulation of photographs has created the contemporary generation of artists. The widespread use of social media today has led illustrators to work in this field.

Computers and software have allowed designers to quickly and easily bypass the design processes that used to take hours and focus on other important areas such as creativity and innovation. With digital methods becoming more common, money and time have also been saved. Computer technology has made it easy to review and edit errors quickly. For this reason, it allowed designers to pay more attention to details. Computers put typesetting tools in the hands of individual designers, giving them a trial period in the design

of new and unusual typefaces and page layouts. The rapid development of technology has also significantly affected the way illustrations are created and distributed to audiences.

Graphics Tablet

Graphic tablets are devices that have a stylus-controlled interface and also have a computer input. Graphic tablets vary according to the technology used. But in general, all graphics tablets use received signals to determine the horizontal-vertical position of the stylus, its distance from the tablet surface, and its inclination. Graphic tablets are widely used among digital illustrators today. It is especially preferred for creating two-dimensional drawings. The pens of graphic tablets can also be used as a mouse. It has a drawing surface that makes up the majority of the surface area of the top of the tablets. This surface is pressure sensitive and records every line and curve the designer draws. Graphic tablets are also used to capture handwritten signatures. The image drawn on the tablet is transferred directly to the computer environment. It is preferred by illustrators because of the flexible movements of digital pens. Drawn images usually do not appear on the tablet itself. Instead, it appears on the computer monitor. After the tablets are connected to the computer, drawing continues by looking at the computer while drawing. Graphics tablets can be used with many different types of software, including graphics, animation, and drawing software. Due to its versatility, it is preferred by engineers and architects as well as designers.

Drawing Tablet

Drawing tablets are an essential tool for artists dealing with digital illustration. It captures drawings accurately and transfers them to digital files to increase work efficiency. Drawing tablets allow users to draw without the need for a computer connection like graphics tablets. It is possible to make precise drawings thanks to the pressure sensitivity with the drawing pen called stylus. The hardness and softness of the lines can be easily adjusted with the pressure to be applied on the drawing with a pencil. With different software and applications, it is possible to give illustrations with digital effects that are done manually in traditional methods. While working with a brush on drawing tablets, the page can be tilted and rotated in all directions in order to achieve a certain stroke.

Drawing Robots

Drawing robots recreate everything drawn on paper on a touchscreen device, using a pen or paintbrush. With drawing robots, it is possible to apply ma-

materials such as watercolor, which are used in traditional methods, on paper. While drawing a real-time watercolor drawing on a computer accompanying application, the robot follows the drawing, dips its brush in water, and then picks up the correct paint color and completes the painting process. According to the drawing robot brand users prefer, it can hold a pencil or paint brush while allowing it to sit securely on a metal plate or piece of paper.

In general, drawing robots capture the same drawing by following the movements of the human hand using software. Due to its ease of use and practicality, its use is rapidly spreading today.

Results and Conclusions

Considering the digitalized world today, the advertising industry also benefits from this area. Advertising is very effective in selling the same type of products that users or consumers can choose from. Advertisements made with effective illustrations, on the other hand, are catchy and attract attention to the product. In addition to advertisements, illustrations are frequently used in children's books. Considering the developmental processes of individuals, such books play important roles in mental development in childhood.

With digitalization, various applications and tools have emerged to transfer illustrations used in graphic design to users. These applications are followed by amateur or professional designers. The process that started with desktop computers has moved to devices small enough to fit in our pockets. The digitalized process is revising itself in a way that changes every day. Especially the current pandemic has led to the advancement of even daily life through digital platforms. The graphic design industry did not remain indifferent to this situation. The fact that the process of shooting the photographs used in the designs was costly and then the processing of the photographs took a long time led the artists to use illustration. The fact that the illustrations are designed and applied to different platforms regardless of time and place has been an indicator of keeping up with the digital world. The fact that illustrations made with vector programs do not have any problems in scaling and can be applied to any surface has been a great advantage for artists. Today, thanks to advanced technology, illustrators also create works that are difficult to distinguish from photographs. In this period when the use of social media is quite common, illustrators compete their arts with interesting projects. In addition, although digital methods are used, traditional methods that have survived from the past to the present are continued. In fact, both species are used together and new species emerge. Traditional methods were abandoned by some artists because they were found to be tedious. When we look at the digital side of the business, the users are too

many to be underestimated. They produce interesting works with the tools provided by technological opportunities.

Illustrations are considered an integral subset of graphic design. Nowadays, it makes a name for itself independently of graphic design. Illustrations, which once competed with photographs and lost this race, occupy a valuable part of our lives today. Although it is not known how the future of illustrations will be shaped by technological developments such as developing software and robotic drawing, it is no doubt that it will continue to exist in the future as it has come from the Paleolithic ages.

References

1. Meyer, U., Schaupp, S., & Seibt, D. (Eds.). (2019). *Digitalization in industry: Between domination and emancipation*. Springer Nature.
2. Liu, J. (2021, April). *Application of Digital Technology Hand-drawn Illustrations in Commercial Posters*. In 2021 International Conference on Computer Technology and Media Convergence Design (CTMCD) (pp. 310-313). IEEE.
3. Husarik, S. (2007). *The impact of digitalization upon the arts and humanities*. International Journal of the Humanities, 5(7).
4. Chu, Y. (2018, October). *Analysis of the Application of Illustration Art in Graphic Design*. In 2018 3rd International Conference on Politics, Economics and Law (ICPEL 2018) (pp. 539-541). Atlantis Press.
5. Ambrose, G., Harris, P., & Ball, N. (2019). *The fundamentals of graphic design*. Bloomsbury Publishing.
6. Klimowski, A. (2012). *On Illustration*. Bloomsbury Publishing.
7. Zeegen, L. (2009). *What is illustration?* RotoVision.
8. Wilson, B. (2016). *The Use and Manipulation of Graphic, Spot News Images: Non-Photographers More Tolerant of Digital Manipulation*. U. Balt. J. Media L. & Ethics, 5, 4.
9. Wood, P. (1994). *Scientific illustration: A guide to biological, zoological, and medical rendering techniques, design, printing, and display*. John Wiley & Sons.
10. Özcan, A., Arman Kandırmaz, E., Türker, N. (2018) *Sectoral impact of web to print applications in printing industry*, In 2018 V. International Multidisciplinary Congress of Euresia, (pp 257-264).

КОМПЛЕКСНЫЙ ПОКАЗАТЕЛЬ КАЧЕСТВА ПЕЧАТИ НА АЛЮМИНИЕВЫХ БАНКАХ

Юраскова И., Проскуряков Н.

Тульский государственный университет

Abstract

Packaging is an integral part of food products sold to the public. Despite the high requirements for the print on an aluminum jar, there is no comprehensive indicator for assessing its quality. Not all indicators of the quality of printing on aluminum jars can be directly measured. Therefore, when determining the quality of aluminum cans, we used the expert assessments method. During the study, 5 specialists selected the following most significant indicators that determine the quality of printing on an aluminum jar: print clarity; color accuracy; technological gap; continuity; uniformity and smoothness. Further analysis consisted in checking the distribution of estimates received from experts; determining the consistency of expert opinions using the coefficient of variation; normalizing ranks, determining the weighting coefficients of each indicator. The resulting comprehensive indicator of print quality assessment can be applied at the stage of quality control of finished aluminum jars, as well as at the acceptance stage, before packing the product.

Key words: *aluminum jar, quality, printing, expert assessment, complex quality indicator.*

Введение

Упаковка является неотъемлемой частью пищевой продукции, реализуемой населению. К упаковке предъявляют следующие основополагающие требования: безопасность, экологичность, надежность, совместимость, взаимозаменяемость, экономическая эффективность, эстетичность.

В рамках Стратегии повышения качества пищевой продукции в Российской Федерации до 2030 года можно выделить следующие основные направления повышения качества пищевой продукции, связанные с упаковкой:

- создание единой информационной системы прослеживаемости пищевой продукции;

- совершенствование системы мониторинга качества, безопасности пищевых продуктов и здоровья населения;
- обязательность внесения в маркировку пищевой продукции обозначения стандарта или документа, в соответствии с которым произведена и может быть идентифицирована пищевая продукция.

Представление результатов исследования (Analysis)

Рассматривая данные актуальные направления можно отметить следующие основополагающие функции упаковки: хранение, транспортировка, и как следствие обеспечение безопасности продукции, а также информационная. В этой связи контроль качества полиграфического покрытия упаковки является важной задачей производства.

В условиях цифровизации сельского хозяйства при развитии концепции циклической экономики следует ожидать снижение привлекательности пластика и увеличение объемов производства тары и упаковки из алюминия [1]. Самую большую долю в жесткой алюминиевой упаковке занимают банки для напитков [2]. Рассмотрим особенности декорирования их поверхности.

Алюминиевые банки для напитков производят методом глубокой вытяжки, из чего следует, что печать заранее не наносится. Поверхность банок декорируют нелитографическим способом по принципу «сухой офсет». На первом этапе наносится грунтовое покрытие для формирования основного белого цвета. Далее на поверхности листа создают негативное изображение. С офсетного вала изображение передается на корпус банки. Количество цветов ограничивается числом отдельных печатающих головок печатной системы и обычно составляет не более 6, а между элементами разного цвета необходим технологический зазор [3], из чего следует, что получить плавные переходы цвета невозможно.

К качеству печати на алюминиевых банках и краскам предъявляют особые требования, так как на последующих производственных этапах горловина банки будет деформироваться с целью придания формы, а также уже затаренные банки подвергаются стерилизации. Несмотря на высокие требования, предъявляемые к отпечатку на алюминиевой банке, нет комплексного показателя для оценки его качества. Разработаем его далее.

При оценке полиграфического покрытия алюминиевой банки не все показатели качества возможно непосредственно измерить, поэтому целесообразно использовать метод оценки, основанный на профессиональном опыте специалистов, либо их групп, у которых имеется за-

пас профессионального, научного или практического опыта, а качество рассматривать как систему экспертных оценок. Такой метод включает процедуры синтеза множественных суждений, получения приоритетности критериев и нахождения альтернативных решений.

К экспертному опросу было привлечено 5 специалистов, которые оценивали 6 критериев. Рассмотрим более подробно отобранные экспертами наиболее значимые показатели, определяющие качество отпечатка на алюминиевой банке далее.

Четкость отпечатка – безусловный показатель качества, нарушение которого бракует изделие. Данный показатель является качественным и оценивается следующим образом:

- если изображения четкие и все надписи читаемы, то $D = 1$;
- если все надписи читаемы, изображения нечеткие, что не портит внешний вид продукции, то $D = 0,5$;
- если надписи не читаемы или отпечаток нечеткий, что портит внешний вид продукции, то $D = 0$.

Точность цветопередачи оценивается в соответствии с образцом-эталоном [4]. Оценка данного показателя визуальна и субъективна, введем следующую градацию:

- если цветопередача соответствует образцу-эталоны, то $C = 1$;
- если цветопередача не соответствует образцу-эталоны, но не портит внешний вид продукции, то $C = 0,5$;
- если цветопередача не соответствует образцу-эталоны и портит внешний вид продукции, то $C = 0$.

Также цвета покрытия не должны изменяться при пастеризации в воде при температуре 70°C в течение 60 минут [4]. Данный показатель не учитывается при составлении комплексного показателя качества, так как он не вариативен.

Между элементами разного цвета необходим технологический зазор, который представляет собой не запечатываемую обводку толщиной 0,1 мм [3]. При запечатывании поверхности банки допускается несовмещение красок до 0,5 мм [5], соответственно эталонное значение для показателя «технологический зазор» $Z = 0,5$ мм.

Сплошность покрытия показывает наличие микроотверстий и степень оголенности металла, вызванную неполным лаковым покрытием. Данный показатель можно оценить с помощью высоковольтных электроискровых дефектоскопов, принцип работы которых основан на фиксации электрического пробоя высоким напряжением, следующим образом:

- если дефекты покрытия на токопроводящих подложках не обнаружены, то $S = 1$.

– если обнаруженные дефекты незначительны и не влияют на качество выпускаемой продукции, то $S = 0,5$.

– если обнаруженные дефекты значительны и влияют на качество выпускаемой продукции, то $S = 0$.

Равномерность и гладкость покрытия определяется отсутствием пузырей воздуха, не пористостей поверхностью и оценивается визуально с помощью увеличительных приборов. Введем следующую градацию для оценки данного показателя:

– если поверхность не пористая, пузыри воздуха отсутствуют, то $E = 1$;

– если поверхность пориста незначительно, что не портит внешний вид продукции, то $E = 0,5$;

– если поверхность пориста и присутствуют пузыри воздуха, то $E = 0$.

По результатам экспертизы была проведена проверка распределения оценок, полученных от экспертов и определена согласованность мнений экспертов с помощью коэффициента вариации (см. табл.), который позволяет определить, какую степень разбросанности имеют значения исследуемого параметра. Значение коэффициента вариации не превышает 40%, следовательно, совокупность считается однородной, можно заключить, что мнения экспертов согласованы в достаточной степени.

Таблица 1. Сводные данные по показателям качества

Показатель	Обозначение	Значение	Коэффициент вариации, %	Степень согласованности	Место фактора по результатам ранжирования	Коэффициент весомости
Четкость отпечатка	D	1	24	средняя	1	0,33
Точность цветопередачи	C	1	19	значительная	5	0,07
Технологический зазор	Z	0,5	34	средняя	4	0,13
Сплошность	S	1	35	средняя	2	0,27
Равномерность и гладкость	E	1	25	средняя	3	0,2

Поскольку задача данного исследования лежит не в области квалиметрического анализа, а скорее в сфере технологических нововведений, касающихся проблемы оценки качества полиграфического покрытия, то допустима упрощенная схема комплексного анализа. В связи с этим расчет комплексного показателя сведется к следующей формуле:

$$K = \sum_{i=1}^n \frac{Q_i}{Q_i^{\text{эт}}} \times q_{K_i}, \quad (1)$$

где K – комплексный показатель,
 Q_i – абсолютное значение i -го показателя свойства,
 $Q_i^{\text{эт}}$ – эталонное значение i -го показателя свойства,
 q_{K_i} – весомость i -го показателя свойства,
 n – количество показателей свойств.

Для оценки достоверности полученных результатов была произведена процедура нормирования, которая заключается в определении численных рамок рангов с последующим вычислением коэффициента конкордации Кендалла и значения критерия Пирсона. Затем для каждого параметра были определены коэффициенты весомости (см. табл.), отражающие количественную характеристику значимости каждого показателя среди других показателей качества. Очевидно, что для выбранной группы экспертов четкость отпечатка – одно из важнейших требований к качеству.

По результатам получена формула для расчета обобщенного комплексного показателя:

$$K = \frac{D}{1} \times 0,33 + \frac{C}{1} \times 0,07 + \frac{(0,5 - Z)}{1} \times 0,13 + \frac{S}{1} \times 0,27 + \frac{E}{1} \times 0,2 \quad (2)$$

где D – четкость отпечатка,
 C – точность цветопередачи,
 Z – технологический зазор,
 S – сплошность,
 E – равномерность и гладкость.

Выводы (Conclusions)

1. В соответствии с полученным на основе метода экспертных оценок комплексным показателем удалось найти пути решения общей проблемы – комплексной оценки качества отпечатка на алюминиевой банке.

2. Разработанную методику рекомендуется применять в производственных условиях на этапе контроля качества готовых алюминиевых банок, а также на этапе приемки, перед затариванием продукта.

Список литературы (List of references)

1. Юраскова, И. А. Актуальность использования алюминия при производстве тары и упаковки для пищевой продукции в условиях цифровизации сельского хозяйства // Тезисы докладов конференции «Промышленная революция 4.0: Взгляд молодежи». Тула: Издательство ТулГУ, 2019. – С. 65–66.
2. Юраскова, И. А. Проскуряков Н.Е. Классификация алюминиевой пищевой упаковки // В сборнике: Полиграфия: технология, оборудование, материалы. Материалы XI научно-практической конференции с международным участием. Редколлегия: С. Н. Литунов [и др.]. Омск: Изд-во ОмГТУ, 2020. – С. 11–17.
3. Осипов, М. Smashing pineapples... [Электронный ресурс] URL: https://www.publish.ru/articles/200910_10761031/ (дата обращения: 24.06.2021).
4. ГОСТ Р 8.827–2013 ГСИ. Метод измерения и определения индекса цветопередачи источников излучения. МКО 013,3–1995 и МКО 177:2007. – М.: Стандартиформ, 2019. – 19 с.
5. ГОСТ 33748–2016 Банки алюминиевые глубокой вытяжки с легко-вскрываемыми крышками. Общие технические условия. – М.: Стандартиформ, 2019. – 24 с.

STUDY OF IMAGE MICRO-LINES REPRODUCTION QUALITY ONTO DIGITAL OFFSET PRINTING PLATES

Sajek D., Valčiukas V.
Kaunas University of Applied Sciences

Abstract

The quality of reproduction of binary image elements in the computer-to-plate systems is very important for high quality of prints. Accurate reproduction of printing elements is of a particular importance in order to print a wide range of high-quality documents with fine image elements or micro-lines. This paper presents the results obtained from the study on the quality of the micro-line reproduction using computer-to-plate systems and thermo-sensitive printing forms produced in these systems applying IR (infrared, 830 nm wavelength) laser technologies.

The quality of reproduction of micro-lines on the printing forms, as well as on the final version of the printed document on the print material, is determined by a number of factors such as parameters of the computer-to-plate recording system, properties of the printing forms, etc. The aim of this study is to evaluate the quality and accuracy of the reproduction of the micro-lines taken into consideration the nature of the printing forms when the micro-lines are arranged parallel or perpendicular to the direction of the image recording.

Keywords: *offset printing form, thermo-sensitive printing plate, binary image element, image micro-line, computer-to-plate system.*

Introduction

Modern computer-to-plate systems designed for the production of offset printing forms use a variety of printing plates, which differ in their physical, chemical and structural properties. Under production conditions, this complicates the optimal selection of the printing plates when it is important to ensure high print quality for a particular segment of the printed production. The choice is also complicated by the fact that it is necessary to take into consideration not only types of the printing plates and their technological properties, but also to evaluate the capabilities of the printing form production equipment. The properties of the printing plates and technical parameters of the printing form production equipment define integral characteristics

of the printing forms quality such as image gradation, its range, reproduction accuracy of graphic image elements, minimal sizes of the image elements, width of micro-lines, including differently oriented on the printing forms, e.g. arranged in parallel and perpendicular direction of the image recording, etc. (Caek et al, 2017; Sajek, 2014).

Under production conditions, the use of Digital Control Wedges for printing forms is insufficient to define the quality of the image elements reproduction on the printing forms. In order to reliably predict reproduction quality of different sized image elements on the specific type of the printing forms using the specific parameter's device, modulation transfer function can be applied (Caek et al, 2017; Андреев, 2007).

The study is aimed to analyse the properties of the offset positive thermo-sensitive printing plates widely used in the printing industry when the image is recorded in a computer-to-plate device using IR wave laser. The paper presents the results obtained from the study on integral quality indices of the printing forms e.g. differently oriented micro-lines on the printing form. In the course of the study, the impact of the selected recording mode on the reproduction accuracy of the different orientation micro-lines was determined.

Material and Methods

In the course of the study, the reproduction of image micro-lines on thermo-sensitive printing plates *Fuji LH-PCE Brillia* and *Fuji LH-PJE* were analysed. Computer-to-plate equipment *Creo Trendsetter 800 Quantum* and *Creo Lotem 800* were used to record the image on the printing plates. The obtained experimental data were used to evaluate technological capabilities of printing plates. In addition, the impact of the image recording parameters on reproduction-graphic characteristics of the printing plates were assessed.

The printing plate *Fuji LH-PCE Brillia* was used for the positive image recording e.g. the active non-printing image element is formed as the result of thermo-destruction process when the layer is exposed to IR radiation. Later on, this layer is removed during the development process. The manufacturer indicates high technological and reproduction-graphic indices. In the presence of screening liner of 200 lpi, the minimum width of a reproducible stroke line is specified at 13 μm . On this plate, a special digital image control strip was recorded in *Creo Trendsetter 800 Quantum* plate-setter with micro-lines arranged parallel and perpendicular to the recording direction. On the digital image control strip were arranged separate micro-lines (their width ranging from 10 to 35 μm , when a step equal to 5 μm), in addition to linear structures that form periodic grids designed to determine resolution.

The width of the recorded micro-line was 10 μm and 15 μm , accordingly. In addition, 100 μm width micro-lines were recorded.

In the course of the experiment, the variable parameter was power of the laser imaging head which varied from 11 kW to 21 kW (a step equal to 1 kW; the total laser power is indicated here and elsewhere). Drum rotation speed (230 rpm), image recording resolution (2400 dpi) and screening liner (150 lpi) were constant parameters. A digital image control strip was recorded in stages starting at 11 kW. Using this method, a digital image control strip was recorded 11 times in 11 different modes. After recording, a printing form was developed. Prior to the measurements, gum solution was washed away from the printing form surface. The width of micro-lines was measured with a scanning electron microscope *Quanta 200* which resolution is 10 nm, enabling to magnify the image up to 10^5 times.

Under production conditions, image recording onto certain types of printing plates occurs by setting a constant parameter of laser radiation intensity. The intensity is altered if the printing plates are changed e.g. thermo-sensitive form material with different technical characteristics is chosen. In this case, after evaluating sensitivity to radiation of the form material, software installed in the form production equipment selects intensity of laser radiation suitable for printing plates of a particular type.

Results

While recording an image onto *Fujifilm LH-PCE* printing plates in the *Creo Trendsetter 800 Quantum* plate-setter, taking into consideration the sensitivity (170 mJ/cm^2) of these plates, it is important to ensure adequate energy density which corresponds to laser power of 16 kW. The width of micro-lines was measured on the printing form recorded using the above-mentioned power, and the obtained results are presented in Table 1 and Table 2. The results showed that micro-lines in the periodic grid are reproduced with significant geometrical inaccuracies (see Table 1). Inaccuracies are more significant of wider micro-lines arranged perpendicular to the recording direction, in contrast to the micro-lines of the same width arranged parallel to the recording direction. Fine separately arranged micro-lines (see Table 2) are reproduced with larger distortions when they are arranged parallel to the recording direction.

*Table 1. Width of reproduced micro-lines of the periodic grid.
Printing form Fuji LH-PCE, 16 kW*

Micro-line orientation	Parallel to the recording direction			Perpendicular to the recording direction		
	10	15	100	10	15	100
<i>Micro-line width in the file, μm</i>						
<i>Micro-line width on the printing form, μm</i>	7,6	11,42	98,29	8,10	11,93	97,2

*Table 2. Width of reproduced individually arranged micro-lines.
Printing form Fuji LH-PCE, 16 kW*

Micro-line orientation	Parallel to the recording direction		Perpendicular to the recording direction	
	10	15	10	15
<i>Micro-line width in the file, μm</i>				
<i>Micro-line width on the printing form, μm</i>	8,89	11,92	9,63	12,46

In addition, the micro-lines of 10, 15 and 100 μm width arranged in the periodic grid parallel and perpendicular to the recording direction were measured on the printing form (see Table 3 and Table 4).

Table 3. Width of the periodic grid micro-lines arranged parallel to the recording direction. Printing form Fuji LH-PCE

Micro-line width in the file, μm	Laser power, kW					
	11	13	15	17	19	21
	Micro-line width on the printing form, μm					
10	9,04	8,20	7,84	7,64	7,12	6,84
15	14,82	13,24	11,76	11,06	9,92	8,68
100	100,85	99,57	98,51	97,87	96,84	95,4

Table 4. Width of the periodic grid micro-lines arranged perpendicular to the recording direction. Printing form Fuji LH-PCE

Micro-line width in the file, μm	Laser power, kW					
	11	13	15	17	19	21
	Micro-line width on the printing form, μm					
10	9,64	7,58	8,27	7,89	7,19	7,56
15	10,29	8,97	8,77	8,31	8,12	7,80
100	99,92	98,52	97,87	96,68	95,67	94,01

Based on the measurement data and chart (see *Figure 1*), it is obvious that the accuracy of reproduction in the periodic grid of 100 μm width micro-lines on this type of positive printing forms depends on the laser intensity and the direction of micro-lines arrangement. As the laser intensity increases, the width of micro-lines arranged parallel to the recording direction decreases, yet not so significantly, in comparison to micro-lines arranged perpendicular to the recording direction. Thus, it can be stated that the quality of reproduction of 100 μm width micro-lines is higher when they are arranged on the printing form parallel to the recording direction.

The width of 10 and 15 width micro-lines on the periodic grid decreases as laser intensity increases due to the direction of thermal energy diffusion, from directly exposed active non-printing areas to passive printing areas. These fine micro-lines are reproduced more accurately as they are arranged perpendicular to the recording direction.

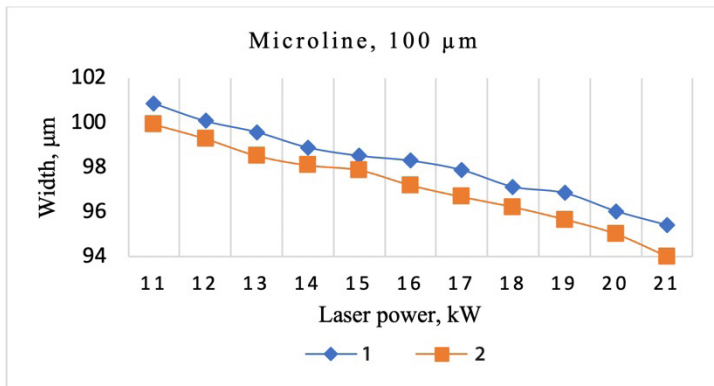


Figure 1. Dependence of the 100 μm width micro-lines variation of the periodic grid on laser power. 1 – parallel arrangement to the recording direction; 2 – perpendicular arrangement to the recording direction. Printing form Fuji LH-PCE

Separate strokes of 10 and 15 μm arranged parallel and perpendicular to the recording direction were measured (see *Table 5* and *Table 6*)

Table 5. Width of the separately arranged micro-lines parallel to the recording direction. Printing form Fuji LH-PCE

Micro-line width in the file, μm	Laser power, kW					
	11	13	15	17	19	21
	Micro-line width on the printing form, μm					
10	11,08	10,21	9,32	8,70	8,29	7,31
15	14,23	13,15	12,21	11,61	10,97	10,21

Table 6. Width of the separately arranged micro-lines perpendicular to the recording direction. Printing form Fuji LH-PCE

Micro-line width in the file, μm	Laser power, kW					
	11	13	15	17	19	21
	Micro-line width on the printing form, μm					
10	11,65	10,75	9,83	9,32	8,58	7,84
15	14,42	13,42	12,72	11,98	11,03	10,54

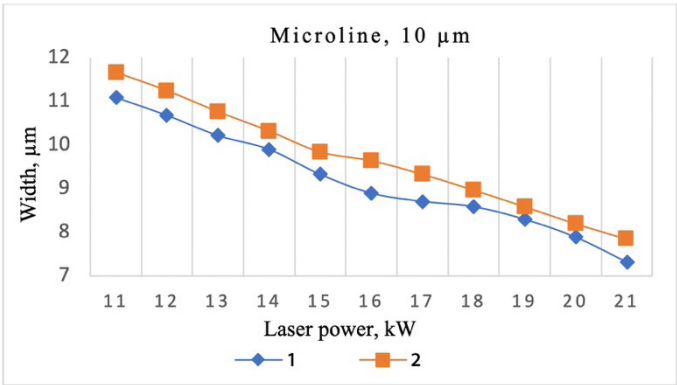


Fig 2. Dependence of the width variation of 10 μm micro-lines of the periodic grid on laser power. 1 – parallel arrangement to the recording direction; 2 – perpendicular arrangement to the recording direction. Printing form Fuji LH-PCE

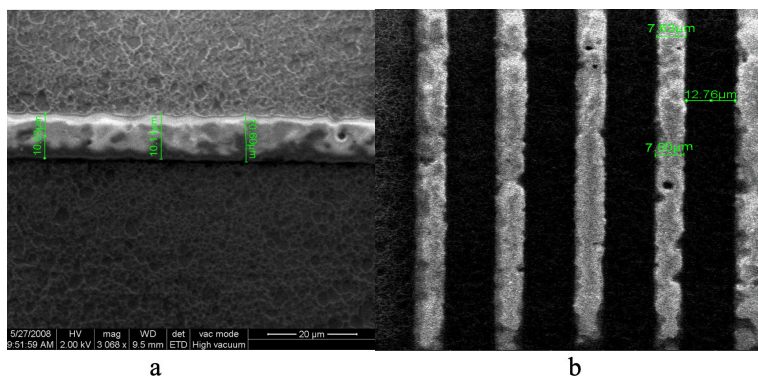


Figure 3. Micro photography of the 10 μm micro-lines: a – separate line;
b – a periodic grid. Printing form Fuji LH-PCE

In order to confirm or refute the obtained results, the accuracy of the micro-lines reproduction on the thermo-sensitive positive printing plates/*Fuji LH-PJE*, which were recorded in the *Creo Lotem 800* device, were evaluated analogously. During this experiment, laser intensity and drum rotation speed were altered. By altering one or another parameter, the amount of energy reaching the plate surface is changed at the same time changing the size of image elements (Caek, Валчюкас, 2011).

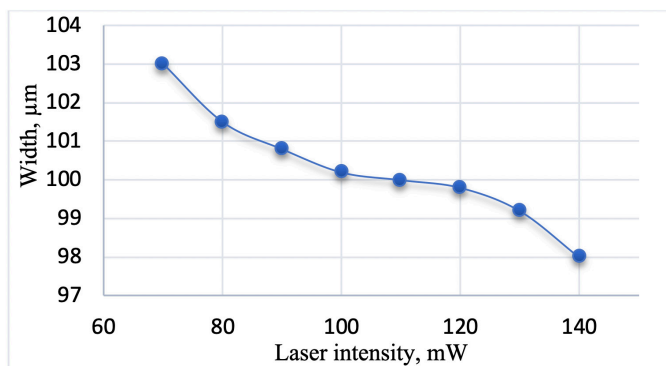


Fig 4. Dependence of the width variation of 100 μm micro-lines of the periodic grid on laser intensity, as lines are arranged perpendicular to the recording direction. Printing form Fuji LH-PJE, drum speed 900 rpm

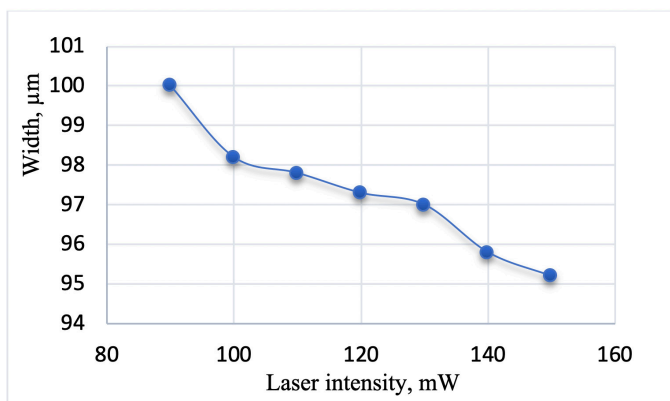


Figure 5. Dependence of the width variation of 100 μm micro-lines of the periodic grid on laser intensity, as lines are arranged parallel to the recording direction. Printing form Fuji LH-PJE, drum speed 900 rpm

As the obtained results show, the accuracy of reproduction of 100 μm width micro-lines is higher, if the micro-lines on the printing form are arranged parallel to the recording direction. In the presence of the optimal amount of energy, fine micro-lines of this type of the printing form are less distorted when they are arranged perpendicular to the recording direction.

Conclusions

The results of the study of the reproduction of fine image details (micro-lines) on the offset digital thermo-sensitive positive printing plates in the computer-to-plate systems showed that the width of recorded micro-lines depends not only on the laser intensity, drum rotation speed or physical and chemical properties of the printing plates, but also on orientation of the printing elements onto the printing form and the image recording direction at the computer-to-plate system.

The results of the study on the accuracy of reproduction of the micro-lines using printing plates Fuji LH-PCE Brillia and Fuji LHPJE showed the dependence of the reproduction quality on the orientation of printing elements on the printing form and the image recording direction.

In terms of the periodic grid of micro-lines, the wider micro-lines (100 μm width and up) are reproduced with significant inaccuracies, given the micro-lines are arranged perpendicular to the recording direction. Wider

micro-lines if they are arranged parallel to the recording direction are reproduced more accurately (see *Table 1, 3, 4*).

Fine individual micro-lines arranged parallel to the recording direction are reproduced not so accurately as fine micro-lines arranged perpendicular to the recording direction (see *Table 5* and *Table 6*).

The results correlate with previous studies of the quality of reproduction of image elements of offset thermo-sensitive printing forms (Sajek, 2014; саек, Валчюкас, 2011; Арутюнова et al, 2009). The obtained results can be applied in optimizing production processes of offset printing forms in order to achieve high-quality printed production.

References

1. Саек Д., Карташева О. А., Андреев Ю. С. Обзор и применение методов оценки интегральных показателей качества офсетных печатных форм (2017). Известия Тульского государственного университета. Технические науки. Выпуск 9-1. ISSN 2071-6168, 356–365.
1. Андреев, Ю. Функция передачи модуляции для оценки полиграфических репродукционных систем (2007). Полиграфия (4), 30–32.
2. Арутюнова, С., Карташева О., Саек Д. Оценка функции передачи модуляции системы цифровой записи офсетных печатных форм (2009). *Proceedings of International Conference „Innovations of publishing, printing and multimedia technologies*, 14–18.
3. Sajek, D. Analysis of Geometrical Measurements of Graphic Elements onto Digital Offset Printing Forms Agfa Energy Elite Pro (2014). *Proceedings of International Conference „Innovations in publishing, printing and multimedia technologies”*, 64–71.
4. Саек, Д., Карташева, О., Андреев, Ю. Обзор и применение методов оценки интегральных показателей качества офсетных печатных форм (2017). Известия Тульского государственного университета. Технические науки. Выпуск 9-1. ISSN 2071-6168, 356–365.
5. Саек, Д., Валчюкас, В. Оценка функции передачи модуляции системы цифровой записи на термочувствительные офсетные формные пластины (2011). *Proceedings of International Conference “Innovations of publishing, printing and multimedia technologies”*, 49–57.

INVESTIGATION OF THE FLAME-RETARDANT PROPERTY OF SILICA NANOPARTICLES RATIO IN THE PAPER COATING

Tutak D., Ozcan A., Kandirmaz E.A.

Marmara University, School of Applied Sciences

Abstract

Papers have a highly flammable property and can easily catch fire. This is a major disadvantage for paper and paper packaging materials. For this reason, this can be delayed or prevented by producing papers with high heat resistance. For this purpose, coating formulations containing 1%, 2.5%, 5% and 10% silica nanoparticles were prepared and applied on 80 g/m² office paper. Chemical analyses of the coatings were made with ATR-FTIR. Surface contact angle and surface energy properties of coatings were measured using PocketGoniometer PGX+, gloss measurements of coated papers were carried out with BYK Gardner GmbH micro gloss and color measurements were determined using X-Rite eXact spectrophotometer. Also, absorbency, surface morphology, and limited oxygen index (LOI) of the coatings were determined. All papers were printed with Toyolife LF - 1600 process magenta commercial offset printing ink using an IGT C1 offset printability test device. As a result, it was determined that the contact angle increased and the printability improved. It has been observed that silica nanoparticles coated papers have flame retardant and very good hydrophilicity and their printability values are in accordance with ISO 12647-2.

Keywords: Paper coating, nanoparticles, silica, flame retardant

Introduction

Paper is a porous fiber network with a smooth surface, optical properties, usually coated with various materials, which provide good printing performance. A coating formulation to be applied on paper consists of three main components. It contains mineral pigments to provide optical properties, latex binders for adhesion and strength properties, and polymer additives to adjust runnability during the coating process and to better tune coated paper properties (dispersants, biocides, pH controllers, dyes and foam controllers etc.) (Preston et al., 1993; Ortner et al., 2018; Wedin et al., 2006; Özcan et al., 2018).

Every process and component made during papermaking directly or indirectly affects its physical and surface properties, such as printability, gloss, opacity, fiber orientation, filler and fine content, sizing process, calender nip pressure and coating (Sharma et al. 2020; Ozcan, and Tutak, 2020). Paper surface coating is a process in which a layer with a smooth surface is obtained by coating cellulosic fibers and filling the gaps between them with binders (often starch and/or synthetic latex), pigments and other fillers. The surface coating process is followed by drying and polishing processes. These processes are done to obtain a paper with better sizing, printing and barrier properties (Sharma et al., 2020; Howard and Hodgson, 2015). In addition, surface sizing is an efficient way to improve the water repellency and mechanical properties of paper, which are closely related to the application performance of paper-based products (Ni et al., 2021).

Some products produced in the printing industry are used where high heat resistance is required. For example, when used with the flame-retardant paper in rare books in libraries, the burning of these books during a fire can be delayed. Besides, some products produced in the printing industry are also used at home. Such as printed packages, wallpapers, newspapers etc. are products of the printing industry. The flame-retardant feature of such products ensures that the fire can be extinguished before it increases, due to its delayed ignition feature in a possible fire (Ozcan et al., 2020).

Material and Methods

Coatings were prepared by using nano silica in four different ratios (1%, 2,5%, 5% and 10%) except natural starch. (10% Nano silica coating could not be prepared due to gelling of silica) All prepared coating formulations were applied on 80g/m² office paper. A K-Control laboratory rod coater used for coatings. After coating, the samples were air dried and conditioned according to TAPPI standards. Toyolife LF - 1600 process magenta ink was printed on the surface of papers with IGT-C1 offset tester according to ISO 12647-2 standard. X-Rite manufacturing standards are used for all spectrophotometric and densitometric measurements (according to 0/45° geometry with 2° observer angle with D50 light source in the range of 400–700 nm and 23°C +/- 1°C temperature, 40-60% RH). The difference between the colors of the prints is calculated according to the formula 1 (according to the CIEDE 2000 standard, ISO 13655). Gloss values were measured at 60° according to ISO 2813:2014 standard for printed papers and 75° according to TAPPI standard T480:2005 for unprinted papers. Surface tension values were measured according to ASTM D5946 method.

$$\Delta E^* = \sqrt{\left(\frac{\Delta L'}{k_L S_L}\right)^2 + \left(\frac{\Delta C'}{k_C S_C}\right)^2 + \left(\frac{\Delta H'}{k_H S_H}\right)^2} + R_T \frac{\Delta C'}{k_C S_C} \frac{\Delta H'}{k_H S_H} \quad (1)$$

Results

Starch and different ratio of Nano silica used in coatings have shown different behaviors for CIEL*a*b*, surface contact angle and surface energy, paper and print gloss, limited oxygen index (LOI). The results obtained from the coatings and printings are presented in tables and graphics below.

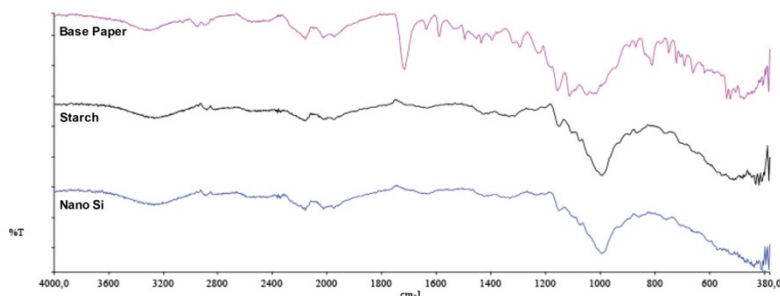


Fig 1. ATR-FTIR spectra of base paper, starch coated paper, silica nanoparticles coated paper

The strong absorption band at 3447 cm^{-1} of silica nanoparticles indicated that -OH on the surface of silica. The characteristic absorptions bands about 1100 cm^{-1} , 810 cm^{-1} , and 470 cm^{-1} were attributed to the asymmetric stretching vibration, symmetric stretching vibration, and bending vibration of Si-O-Si, respectively. When the starch coated papers spectra were examined the strong absorption peak at 3413 cm^{-1} was assigned to the hydrogen bonds association in -OH groups. The bands at 1168 cm^{-1} and 1071 cm^{-1} were attributed to the stretching vibration of C-O in C-O-H groups, and the band at 1026 cm^{-1} was attributed to the stretching vibration of C-O in C-O-C groups. The other characteristic absorptions of starch also appeared at 1463 cm^{-1} , 1408 cm^{-1} , and 860 cm^{-1} .

When the FTIR spectrum of the paper is examined, around 3400 cm^{-1} -OH bands belonging to cellulose the band at 2894 cm^{-1} is attributed to CH stretching vibration of all hydrocarbon constituents in polysaccharides. Typical bands assigned to cellulose were observed in the region of $1630 - 900\text{ cm}^{-1}$. The peaks located at 1633 cm^{-1} correspond to vibration of water molecules absorbed in cellulose. The absorption bands at 1428 , 1367 ,

1334, 1027 cm^{-1} and 896 cm^{-1} belong to stretching and bending vibrations of $-\text{CH}_2$ and $-\text{CH}$, $-\text{OH}$ and $\text{C}-\text{O}$ bonds in cellulose. The reason why the three spectra are very similar to each other is that the peaks of the paper main structure are much more dominant than the others. The results obtained are compatible with the literature (Tang et al., 2009; Hospodarova et al., 2018).

Table 1. Total surface energy and contact angle values according to ASTM D5946 method.

Coating type	Contact Angle	Surface Energy (mj/m^2)
Base	8.8	35.5
Starch	42.6	49.7
1% Nano Silica	29.6	54.4
2.5% Nano Silica	24.2	56.3
5% Nano Silica	18.7	58.3

When looking at the contact angle and surface energy values obtained as a result of the measurement of the surface coatings, it was determined that the filling material used starch reduces the contact angle of the coating, but it increases the surface energy. In contrast to starch, the contact angle of the coating used %5 Nanosilica is the lowest, but it has the highest surface energy. In addition, as the Nanosilica ratio increased in the coating formula, the contact angle increased and the surface energy decreased.

Table 2. Paper Gloss and Print Gloss values

	Base	Starch	1% Nano Silica	2,5% Nano Silica	5% Nano Silica
Paper Gloss	3.04	10.7	4.84	5.96	6.33
Printing Gloss	5.92	13.44	5.73	6.24	5.85

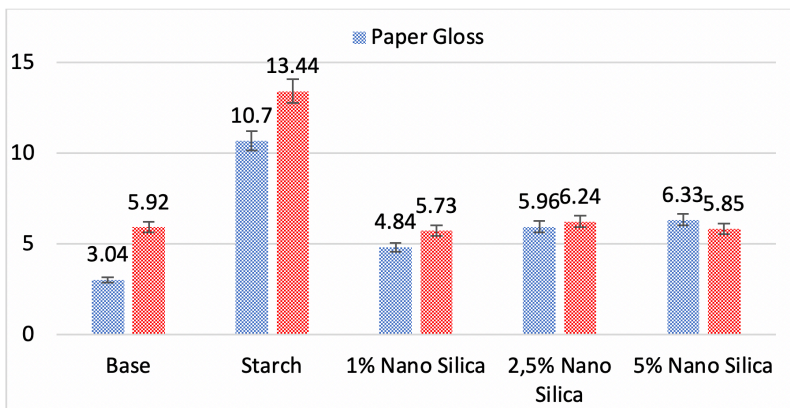


Fig 2. Paper gloss and printing gloss values

The starch applied on the base paper increases both the paper and the printing gloss. In nano silica applied coatings, although the gloss increased a little in both paper gloss and print gloss values, it remained at very low values compared to starch. This is because nano silica creates a roughness on the surface and this causes diffuse reflection and reduces the brightness. However, when starch is used, the increased gloss values are still higher than the untreated paper. This means increased attractiveness of the paper.

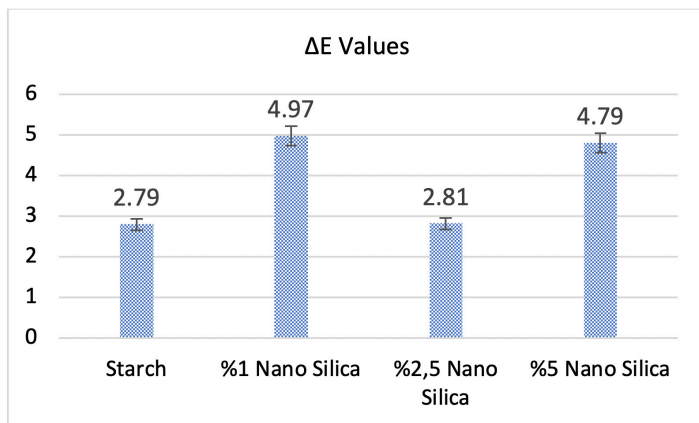


Fig 3. CIE $L^*a^*b^*$ ΔE values

When Delta-E values are compared according to printing parameters, it is seen that Starch and 2.5% Nano Silica ΔE values are lower than the other two coatings. According to ISO 12647-2, values below 5 are acceptable. This shows the acceptability of all coatings in terms of printing. This is because the added nano silica does not glow blue. Nanoparticles glow in different colors depending on their size. This is called the quantum effect. This quantum effect was also observed in the added nano silica. All ΔE values obtained are within the acceptable range specified in ISO 12647-2.

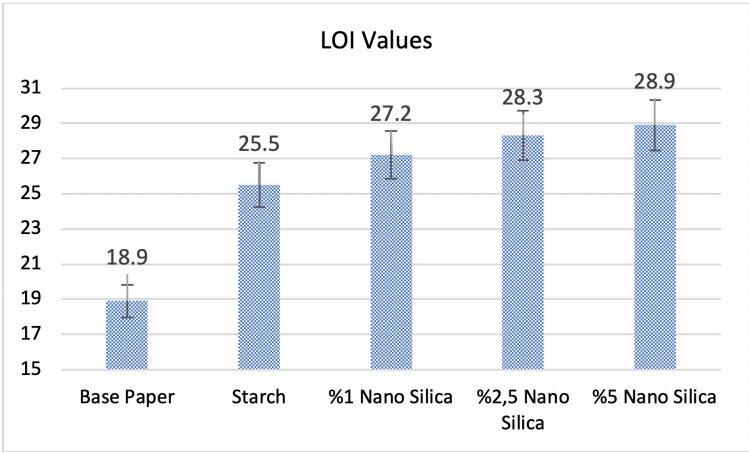


Fig 4. Limited oxygen index (LOI) values of Samples

The flame retardancy properties of nano silica added starch paper coatings were examined with LOI measurements. LOI is a widely used technique to determine the flame retardancy of coatings. LOI values of the coated papers are given in Figure 4. When the figure is examined, the flame retardancy feature is increased by adding nano silica. It was determined that the increase was slightly higher with increasing nano silica amounts. The reason for this increase is that the Si-O-Si bonds on the silica nanoparticle are resistant to increasing temperature and delay the ignition by forming an ash coating on the combustible surface. The obtained results are in line with the literature (Üreyen et al., 2020; Yuan et al., 2017).

Conclusions

While preparing the coating material, mixtures of 1 %, 2.5 % and 5 % were prepared and applied to the paper surface. However, nano silica particles

added to the starch made the mixture into a gel after 5% and could not be used as a coating material.

Starch and Nano silica showed different behaviors both in the optical properties of the paper and in the printing properties.

According to the coating type, in the contact angle and surface energy values, it was determined that as the amount of nano silica in the coating increased, the contact angle decreased and the surface energy increased on the contrary. The low contact angle has a very important value for the offset printing system.

In paper and print glosses, coatings had a positive effect on both paper and print gloss. While paper gloss and print gloss starch coatings have an average of twice the value compared to Nano silica-containing coatings, the ratios are close to each other in Nano silica coatings, although the ratios vary.

When the printing color differences are examined, it has been determined that the printing ΔE values for all coatings are within the acceptable values. It can be said that Starch and 2.5% Nano Silica coatings are better than others.

There were positive changes in the flame-retardant values of the coatings of nano silica particles added to the starch. As the amount of nano silica in the coatings increased, its resistance to flammability also increased. This will ensure that the nano silica included coated papers to be used are more resistant to burning, especially for valuable documents and documents to be stored for a long time.

References

1. Hospodarova, V., Singovszka, E. and Stevulova, N. (2018) *Characterization of cellulosic fibers by FTIR spectroscopy for their further implementation to building materials*. American journal of analytical chemistry, 9(6), 303-310.
2. Howard, K.W. and Hodgson, K.T. (2015) *Influence of pigment packing behavior on the adhesive requirements of aqueous paper coatings*. Journal of Coatings Technology and Research, 12(2), 237-245.
3. Ni, S., Liu, N., Fu, Y., Bian, H., Zhang, Y., Chen, X., Gao, H. and Dai, H. (2021) *Laccase-catalyzed chitosan-monophenol copolymer as a coating on paper enhances its hydrophobicity and strength*. Progress in Organic Coatings, 151, 106026.
4. Ortner, A., Hofer, K., Bauer, W., Nyanhongo, G.S. and Guebitz, G.M. (2018) *Laccase modified lignosulfonates as novel binder in pigment-based paper coating formulations*. Reactive and Functional Polymers, 123, 20-25.

5. Ozcan, A., and Tutak, D. (2020) *The effect of zeolite on inkjet coated paper surface properties and deinking*. Nordic Pulp & Paper Research Journal, 35(3), 432-439.
6. Ozcan, A., Kasikovic, N., Arman Kandirmaz, E., Durdevic, S. and Petrovic, S. (2020) *Highly flame retardant photocured paper coatings and printability behavior*. Polymers for Advanced Technologies, 31(11), 2647-2658.
7. Ozcan, A., Kandirmaz, E.A. and Türker, N. (2018) *Investigation of Printability Properties in Inkjet Printed Coated Papers*. Proceedings- The 5. International Multidisciplinary Congress of Eurasia IMCOFE 2018
8. Preston, D.J., McGenity, P.M. and Husband, J.C. (1993) *The use of rheological techniques in the study of interactions between components of paper coating colours*. Special Publication-Royal Society of Chemistry, 129, 23-23.
9. Sharma, M., Aguado, R., Murtinho, D., Valente, A.J., De Sousa, A.P.M. and Ferreira, P.J. (2020) *A review on cationic starch and nanocellulose as paper coating components*. International journal of biological macromolecules, 162, 578-598.
10. Tang, H., Xiong, H., Tang, S. and Zou, P. (2009) *A starch-based biodegradable film modified by nano silicon dioxide*. Journal of Applied Polymer Science, 113(1), 34-40.
11. Üreyen, M. E., Kaynak, E., and Yüksel, G. (2020) *Flame-retardant effects of cyclic phosphonate with HALS and fumed silica in polypropylene*. Journal of Applied Polymer Science, 137(4), 48308 (1-8).
12. Wedin, P., Svanholm, E., Alberius, P.C. and Fogden, A. (2006) *Surfactant-templated mesoporous silica as a pigment in inkjet paper coatings*. Journal of pulp and paper science, 32(1), 32-37.
13. Yuan, B., Zhang, J., Mi, Q., Yu, J., Song, R., and Zhang, J. (2017) *Transparent cellulose-silica composite aerogels with excellent flame retardancy via an insitu sol-gel process*. ACS Sustainable Chemistry & Engineering, 5(11), 11117-11123.

БИОРАЗЛАГАЕМЫЕ МАТЕРИАЛЫ НА ОСНОВЕ ПЭНП, КРАХМАЛА И МОНОГЛИЦЕРИДОВ

Васильев И.Ю., Ананьев В.В., Черная И.В.
Московский политехнический университет

Abstract

The process of biodegradation of compositions based on LDPE and thermoplastic starch (TPC) of various origin: corn, pea and rice is investigated. Thermoplastic starch was received on the basis of naktivny starches of different types, processing them in laboratory extruders of Brabender and MashkPlast (Russia).

By mixing thermoplastic starches with polyethylene in extruders, biodegradable hybrid compositions (BHA) in the form of strands, granules and films were obtained. Structural parameters of BHA were studied by optical and electron scanning microscopy. The biodegradability of the composite films was evaluated by placing them in biohumus for six months, and during storage, the change in water absorption of the films was determined. Before and after the biodegradation process, tensile fracture stress and elongation at rupture were determined to evaluate the performance of BGC (physical and mechanical characteristics of films). Changes in the chemical structure during biodegradation were determined by Fourier IR spectroscopy.

The positive effect (acceleration of the biodegradation process) from the use of a new type of starch fixers – monoglycerides distilled in TPK/polyethylene compositions – was confirmed. After six months, intensive sporulation of active microorganisms was observed on the surface of the samples. At the same time, water absorption by samples reached 30%, and strength and deformation properties decreased by 60%, which indicates an intensive biodegradation process.

It has been found that the rate of biodegradation depends on the distribution of the natural biodegradable filler in the synthetic polymer composition.

Введение

Уже давно во всем мире серьезную озабоченность вызывает быстрый и практически неуправляемый рост потребления синтетических пластмасс во многих отраслях промышленности, особенно в упаковочной ин-

дустрии [1]. Тару из пластика используют для упаковки пищевых продуктов, лекарственных препаратов, электронных приборов, жидкостей, которые к тому же могут иметь и повышенный класс опасности [2,3].

Серьезное внимание уделяют решению задач повышения качества, надежности и долговечности упаковочных материалов, в основном полимерных пленок, и проблемы их утилизации после завершения срока эксплуатации [4]. Одним из приемлемых способов их решения является создание биоразлагаемых в естественных условиях полимерных материалов [5].

На долю биоразлагаемых материалов в 2021 г. приходится примерно 25–30 % от общего объема рынка пластмасс. Стимул для такого рыночного бума – интерес к инновациям в области упаковки. Согласно результатам исследований European Bioplastics (европейской ассоциации производителей, поставщиков и потребителей биопластиков и других биоразлагаемых материалов), уже в 2007 г. в мире было изготовлено 262 тыс. т биополимеров. При этом 80 % было получено из растительного сырья, 12 % изготовлено из натуральных компонентов, но в естественных условиях не разрушаются; 8 % биопластиков произведено из синтетического сырья и способно к биodeградации [6-10]. Согласно анализу и прогнозам, мировой объем производства и потребления биоразлагаемых упаковочных материалов ежегодно увеличивается на 22 % и эта тенденция сохранится [11–13].

На сегодняшний момент именно биоразложение полимерных материалов, пожалуй, наиболее экологичный способ утилизации отходов упаковки. Интенсивно ведутся работы по разработке биоразлагаемых, компостируемых пластиков на основе природных материалов, не наносящих вреда окружающей среде и здоровью человека [14-15]. Одним из перспективных направлений является создание биологически разрушаемых гибридных композиций (БГК) при использовании термопластичного крахмала (ТПК), как их основного компонента [16, 17].

Для получения ТПК нативный крахмал смешивают при нагревании с различными пластификаторами [18, 23–25]. Показано, что использование в качестве наполнителя полиолефиновых композиций ТПК вместо нативного крахмала обеспечивает лучшую способность к переработке и более высокую термостабильность БГК. При этом содержание в них ТПК может достигать 40–60 масс.% [19, 20].

Целью данной работы является исследование процесса производства и биологической деструкции БГК, наполненных крахмалсодержащими продуктами различного происхождения и модифицированных моноглицеридами дистиллированными (МГД).

Объекты исследования

В качестве объектов исследования использовали:

- полиэтилен низкой плотности (ПЭНП) марки 11503-070 производства ПАО «Казаньоргсинтез» (Россия), со средней молекулярной массой около $1.8 \cdot 10^4$;
- композиционные крахмалосодержащие материалы на основе ПЭ и ТПК;
- глицерин марки ПК-94, плотностью 1.24 г/см^3 производства компании «ТЦ Вымпел» (Россия), ГОСТ 6824-96;
- МГД дистиллированный, произведенный по техническим условиям ТУ 10-1197-95 компанией ООО «РусХимтрейд» (Россия);
- крахмал кукурузный, произведенный ООО «Крахмалопродукт» (г. Орел, Россия) в соответствии с ГОСТ 32159-2013,
- крахмал рисовый – [Vinh Thuan Trading Import-Export Co. Ltd \(Вьетнам\)](#),
- крахмал гороховый – фирмы Roquette (Франция).

Методы исследования

БГК получали на экструдере фирмы «МашПласт» (Россия), оснащенном или стренговой, или плоскощелевой экструзионной головкой при температурах по зонам экструдера от 115 (в зоне загрузки) до 140 °С (в зоне головки) [21].

Физико-механические свойства образцов при растяжении определяли с помощью испытательной машины РМ-50 производства компании «МашПласт» (Россия), оснащенной компьютерным интерфейсом с программным обеспечением «StretchTest». Разрушающее напряжение при растяжении (δ) и относительное удлинение при разрыве (ϵ) БГК измеряли при температуре $23 \pm 2^\circ\text{C}$ и относительной влажности $50 \pm 5\%$ по методу, изложенному в ГОСТ 14236-81. Предел допускаемого значения погрешности измерения нагрузки не превышал $\pm 1\%$. Предельные отклонения по диаметру стренгового и площади пленочного образца составляли $\pm 0,2 \text{ мм}$ и $2\text{--}3\%$ соответственно. Среднее значение определяли по 3–5 измерениям. Испытания проводили при скорости деформации образцов 100 мм/мин. Образцы пленок для испытаний получали с помощью специального вырубного устройства, форма образцов соответствовала типу 1В (ENISO 527-3).

Определение водопоглощения исследуемых БГК проводили в соответствии с ГОСТ 4650-80 «Пластмассы. Методы определения водопоглощения».

Для оценки динамики биоразложения БГК применяли метод компостирования. Образцы помещали в специальные лотки с биогумусом при температуре $23 \pm 2^\circ\text{C}$ и влажности $70 \pm 10\%$ и выдерживали от месяца до полугода. Степень биоразложения полимерных композиций оценивали по изменению физико-механических свойств: разрушающему напряжению при растяжении (σ) и относительному удлинению при разрыве (ϵ), согласно ГОСТ 54530 – 2011.

Оптические исследования внешнего вида БГК после компостирования проводили с помощью микроскопа AxiolmagerZ2m, CarlZeiss (Germany) при увеличении $\times 50$ и $\times 200$ в проходящем и отраженном свете.

Изучение химической структуры БГК осуществляли методом Фурье-ИК-спектроскопии с приставкой МНПВО на приборе ФСМ-1201 (Germany) с разрешением в $1,0 \text{ см}^{-1}$ (спектральный диапазон волновых чисел $375\text{--}7900 \text{ см}^{-1}$).

Результаты и их обсуждение

Проблема создания биоразлагаемых композиционных полимерных материалов заключается в комплексном решении вопросов, связанных как со скоростью их биодеструкции, так и с технологическими, эксплуатационными и другими характеристиками. Одно из требований, предъявляемых к создаваемому материалу – сохранение технологических характеристик, присущих исходному полимеру, что имеет значение для учета возможности его переработки на стандартном оборудовании и в определенных условиях.

На первом этапе работы изготовили БГК на основе ПЭНП и ТПК различного происхождения: кукурузного, горохового и рисового, подобрав оптимальные концентрационные соотношения, в которых доля ТПК составляет от 40 до 60 масс % соответственно [21,22].

Важным этапом исследования является установление сроков биоразложения полученных композиций. Для этого использовали комбинацию нескольких методов: компостирования в биогумусе и оценка водопоглощения.

Сначала оценили водопоглощение БГК образцов. Вода является необходимым компонентом для поддержания жизнедеятельности микроорганизмов. Кроме того, проникая в поверхностные слои, и диффундируя вглубь структуры материала, вода может оказывать пластифицирующее действие.

Результаты исследования водопоглощения представлены в табл.1. Как видно, ПЭНП практически не поглощает воду, в то время как ком-

позиции, наполненные крахмалом, поглощают ее в значительном количестве. Причем, с увеличением содержания ТПК в композициях, увеличивается и водопоглощение. Можно предположить, что это связано со структурными изменениями, протекающими в системе полимер-наполнитель. Происходит разрыхление полимерной матрицы, и увеличивается свободный объем между макромолекулами, что приводит к росту количества поглощенной воды. Наибольшим водопоглощением обладает композиция на основе рисового ТПК. Такая композиция при попадании в почву будет быстрее подвергаться процессу биоразложения.

Таблица 1. Результаты водопоглощения БГК

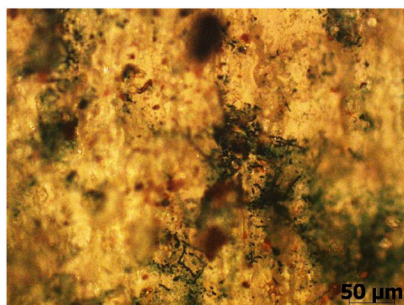
Состав композиции, масс %	Поглощение воды, %
Исходный ПЭНП	0,2
БГК (ТПК:ПЭ кук. кр. 60:40)	7,6
БГК (ТПК:ПЭ кук. кр. 50:50)	4,1
БГК (ТПК:ПЭ кук. кр. 40:60)	2,3
БГК (ТПК:ПЭ гор. кр. 60:40)	7,9
БГК (ТПК:ПЭ гор. кр. 50:50)	3,8
БГК (ТПК:ПЭ гор. кр. 40:60)	2,1
БГК (ТПК:ПЭ рис. кр. 60:40)	8,1
БГК (ТПК:ПЭ рис. кр. 50:50)	5,6
БГК (ТПК:ПЭ рис. кр. 40:60)	2,5

О протекании процесса биоразложения судили по результатам оптической микроскопии, изменениям физико-химических свойств исследуемых материалов по истечении выбранного времени воздействия почвы.

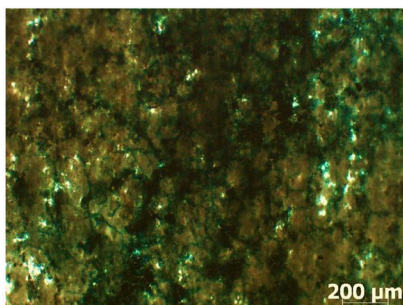
При проведении эксперимента использовали землю, имеющую температуру 23 °С и влажность, соответствующую 70±10 % от ее максимальной влагоемкости. Время компостирования составляло месяц, три месяца и полгода. Образцы БГК и контрольный образец помещали на подложку из почвы и покрывали полностью слоем почвы, при этом обеспечивали постоянный доступ воздуха к образцу во избежание подавления жизнедеятельности микроорганизмов.

На рис. 1 представлены микрофотографии образцов при максимальной массовой доле ТПК:ПЭНП = 60:40 % после полугода нахождения в биогумусе.

1

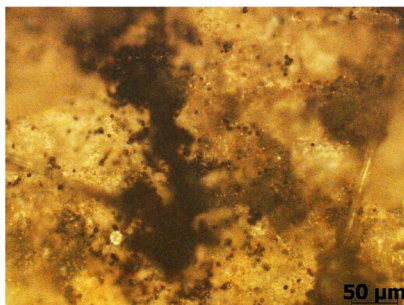


(a)

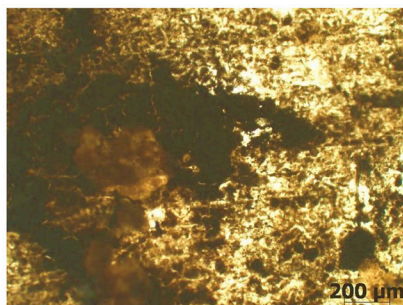


(б)

2

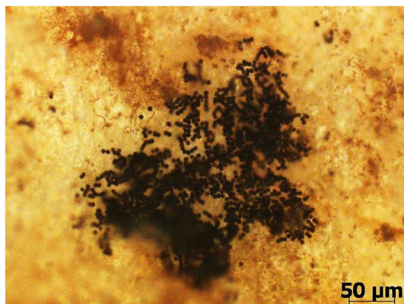


(a)

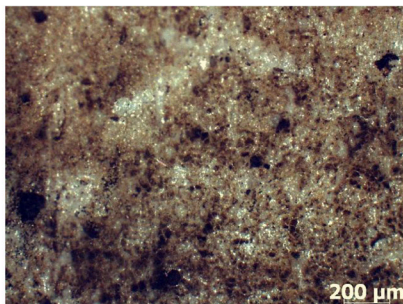


(б)

3



(a)



(б)

Рисунок 1. Микрофотографии пленочных образцов после изъятия из биогумуса

1 – БГК на основе кукурузного крахмала, 2 – БГК на основе горохового крахмала, 3 – БГК на основе рисового крахмала;

а – увеличение $\times 50$, б – увеличение $\times 200$

Как видно из представленных микрофотографий, на поверхности исследуемых композиционных образцов наблюдается локальное развитие почвенных микроорганизмов. Количество введенного ТПК мало влияет на процесс в начальный период, однако динамика роста микроорганизмов на разных образцах при одном и том же количестве ТПК неодинакова. Для образца на основе кукурузного ТПК (1) происходит поверхностное развитие микроорганизмов в виде многочисленных пятен без интенсивного спороношения, в то время как для образцов на основе горохового ТПК (2) и рисового ТПК (3) отчетливо виден сплошной рост микроорганизмов, а также интенсивное спороношение. Наполненные композиции имеют рыхлую структуру и поверхностные дефекты, наблюдается разрушение наполнителя по всему объему образцов.

Результаты определения разрушающего напряжения при растяжении (δ) и относительного удлинения при разрыве (ϵ) для БГК после полугода компостирования представлены в табл. 2.

Как следует из полученных данных, после полугода нахождения исследуемых образцов в биогумусе с почвенными микроорганизмами значения их физико-механических характеристик снижаются. В процессе биоразложения происходит поглощение воды композиционными образцами, вследствие чего происходит изменение структуры материала, энергетические связи, скрепляющие полимерную матрицу и наполнитель, ослабевают. В результате композиции становятся более рыхлыми и хрупкими.

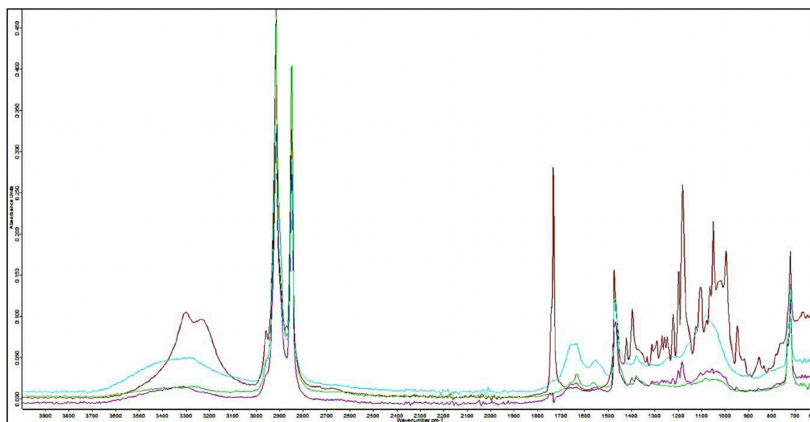
Так, для БГК на основе кукурузного крахмала происходит изменение физико-механических свойств в 1,5 раза, для БГК на основе горохового крахмала – в 1,3 раза, для БГК на основе рисового крахмала – в 2,1 раза. Это позволяет сделать заключение, что в условиях утилизации последних пленочных композиций период их биоразложения будет короче.

Для дополнительной оценки изменений, произошедших в процессе биоразложения, определяли спектральные характеристики, используя метод Фурье-ИК-спектроскопии. В качестве примера, на рис. 2., представлен спектр БГК на основе рисового ТПК при соотношении ТПК:ПЭНП = 60:40 % до и после процесса биоразложения.

В первую очередь представляет интерес оценка интенсивности полос поглощения ОН-групп, расположенных между 3000 и 3600 см^{-1} , и полос между 1000–1500 см^{-1} , характерных для CH_2 , CH_3 и С-О групп. Средняя и дальняя области ИК-спектра менее информативны. Они позволяют фиксировать наличие в составе БГК – ПЭ, функциональных групп, характерных для жирных кислот, которые входят в состав МГД,

*Таблица 2. Результаты физико-механических испытаний БГК
до и после процесса биоразложения*

№ п/п	Соотношение ТПК:ПЭ	σ, МПа (Δ±0.2)	ε, % (Δ±5)	σ, МПа (Δ±0.2)	ε, % (Δ±5)
1.	Исходный ПЭНП	16	195		
		с МГД до биоразложения		С МГД после биоразложения	
2.	ТПК на кукурузной основе				
	60:40	10,9	78	7,2	45
	50:50	11,6	84	8,3	67
	40:60	12,8	93	10,3	84
3.	ТПК на гороховой основе				
	60:40	7,8	82	5,6	48
	50:50	9,3	91	8,4	64
	40:60	10,1	102	9,3	86
4.	ТПК на рисовой основе				
	60:40	11,2	96	5,2	41
	50:50	11,9	104	7,3	56
	40:60	12,8	115	8,9	87



*Рисунок 2. ИК – спектр БГК композиции на основе рисового крахмала
Красный спектр поглощения – БГК до процесса биоразложения, фиолетовый
спектр – БГК после месяца процесса биоразложения, зеленый – БГК после
трех месяцев биоразложения, голубой – БГК после полугода биоразложения*

спиртосодержащих групп, которые относятся к глицерину, а также функциональных групп, относящихся к крахмалу.

После полугода нахождения БГК в биогумусе в ИК спектре появляются пики поглощения в области $1000\text{--}1200\text{ см}^{-1}$ и $1500\text{--}1700\text{ см}^{-1}$, что говорит о проявлении действия активных микроорганизмов, которые образуют бактериальную микрофлору. В области $3000\text{--}3600\text{ см}^{-1}$ происходят изменения интенсивности пика. Это связано с тем, что ТПК, влияя на полимерную матрицу, разрушает ее, и, скорее всего, вымывается водой из композиции. Это позволяет сделать вывод об интенсивном протекании процессов биоразложения.

Заключение

Провели процесс биоразложения БГК композиций на основе ПЭНП и ТПК различного происхождения: кукурузного, горохового и рисового, при содержании ТПК в БГК от 40:60 масс % с использованием нового пластификатора – моноглицеридами дистиллированными. Процесс воздействия биогумуса проводили в течение полугода, с периодической оценкой свойств контрольных и рабочих образцов через месяц, три месяца и полгода.

Из результатов эксперимента следует, что спустя полгода вводимый в состав образцов новый модификатор увеличивает водопоглощение наполненных композиций для БГК на основе кукурузного ТПК – на 20 %, для БГК на основе горохового ТПК – на 26 %, для БГК на основе рисового ТПК – на 31 %.

Физико-механические характеристики образцов при этом снижаются на 60% по сравнению с исходными величинами, видимо, вследствие изменения структуры материала: ослабления энергетических связей, разрушения полимерной матрицы, частичного вымывания компонентов из системы.

Результаты оптической микроскопии подтвердили протекание спороношения активных микроорганизмов, что подтверждает и анализ, проведенный методом Фурье-ИК-спектроскопии.

На основании полученных данных можно сделать вывод о перспективности использования ТПК с новым пластификатором – моноглицеридами дистиллированными, в качестве модификатора полиолефинов для создания упаковочных материалов с приданием им свойства биоразлагаемости.

Примечание: Исследование проводилось при финансовой поддержке РФФИ (Российского фонда фундаментальных исследований) в рамках научного проекта № 19-33-90284\19.

Список используемых источников

1. Литвяк В.В. [Перспективы производства современных упаковочных материалов с применением биоразлагаемых полимерных композиций. Журнал Белорусского государственного университета. Экология. 2019. № 2. С. 84-94.](#)
2. S. Kalia, Biodegradable Green Composites. John Wiley & Sons, 2016. 368 p.
3. Bio-based Building Blocks and Polymers – Global Capacities, Production and Trends 2019 – 2024. Hürth, Germany, Michael Carus (V.i.S.d.P.). – 2020.
4. В.В. Ананьев, П.П. Куликов, И.Ю. Васильев. Исследование полиолефиновых композиций, способных к разложению. Журнал Packaging. 2015. №3. С. 46-48.
5. Nahid Nishat, Ashraf Malik. Synthesis, spectral characterization thermal stability, antimicrobial studies and biodegradation of starch–thiourea based biodegradable polymeric ligand and its coordination complexes with [Mn(II), Co(II), Ni(II), Cu(II), and Zn(II)] metals. [Journal of Saudi Chemical Society Volume 20, Supplement 1](#), September 2016, Pages S7-S15. <https://doi.org/10.1016/j.jscs.2012.07.017>.
6. Y.N.Sudhakar, M.Selvakumar. Lithium perchlorate doped plasticized chitosan and starch blend as biodegradable polymer electrolyte for supercapacitors. [Electrochimica Acta. Volume 78](#), 1 September 2012, Pages 398-405. <https://www.sciencedirect.com/science/article/abs/pii/S0013468612009723>.
7. J.F.Mendes, R.TPaschoalin, V.B.Carmona, Alfredo R Sena Neto, A.C.P.Marques, J.M.Marconcini, L.H.C.Mattoso, E.S.Medeiros, J.E.Oliveira. Biodegradable polymer blends based on corn starch and thermoplastic chitosan processed by extrusion. [Carbohydrate Polymers Volume 137](#), 10 February 2016, Pages 452-458. <https://doi.org/10.1016/j.carbpol.2015.10.093>.
8. Dang MaoNguyen, Thi Vi ViDo, Anne-CecileGrillet, HuyHa Thuc, Chi NhanHa Thuc. Biodegradability of polymer film based on low density polyethylene and cassava starch. [International Biodeterioration & Biodegradation. Volume 115](#), November 2016, Pages 257-265. <https://doi.org/10.1016/j.ibiod.2016.09.004>.
9. Xiaozhi Tang, Sajid Alavi. Recent advances in starch, polyvinyl alcohol based polymer blends, nanocomposites and their biodegradability. [Carbohydrate Polymers. Volume 85, Issue 1](#), 22 April 2011, Pages 7-16. <https://doi.org/10.1016/j.carbpol.2011.01.030>.

10. RahulSingh, RukmaniSharma, MohdShaqib, AnjanaSarkar, Krishna DuttChauhan. Chapter 10 - Biodegradable polymers as packaging materials. [Biopolymers and their Industrial Applications](#). From Plant, Animal, and Marine Sources, to Functional Products. 2021, Pages 245-259. <https://doi.org/10.1016/B978-0-12-819240-5.00010-9>.
11. E.Ojogbo, E.O.Ogunsona, T.H.Mekonnen. Chemical and physical modifications of starch for renewable polymeric materials. [Materials Today Sustainability Volumes 7–8](#), March 2020, 100028. <https://doi.org/10.1016/j.mtsust.2019.100028>.
12. N Tudorachi, C.N. Cascaval, M Rusu, M Pruteanu. Testing of polyvinyl alcohol and starch mixtures as biodegradable polymeric materials. [Polymer Testing. Volume 19, Issue 7](#), August 2000, Pages 785-799. [https://doi.org/10.1016/S0142-9418\(99\)00049-5](https://doi.org/10.1016/S0142-9418(99)00049-5).
13. Abril Fonseca-García, Enrique Javier Jiménez-Regalado, Rocio Yaneli Aguirre-Loredo. Preparation of a novel biodegradable packaging film based on corn starch-chitosan and poloxamers. [Carbohydrate Polymers. Volume 251](#), 1 January 2021, 117009. <https://doi.org/10.1016/j.carbpol.2020.117009>.
14. Aanchal Mittal, Sangeeta Garg, Shailendra Bajpai. Fabrication and characteristics of poly (vinyl alcohol)-starch-cellulosic material based biodegradable composite film for packaging application. Materials today: proceedings. [Volume 21, Part 3](#), 2020, Pages 1577-1582. <https://doi.org/10.1016/j.matpr.2019.11.210>.
15. Shazia Tabasum, Muhammad Younas, Muhammad Ansab Zaeem, Irfan Majeed, Muzamil Majeed, Aqdas Noreen, Muhammad NaeemIqbal, Khalid Mahmood Zia. A review on blending of corn starch with natural and synthetic polymers, and inorganic nanoparticles with mathematical modeling. [International Journal of Biological Macromolecules Volume 122](#), 1 February 2019, Pages 969-996. <https://doi.org/10.1016/j.ijbiomac.2018.10.092>.
16. Лукин Н.Д., Колпакова В.В., Усачев И.С., Сарджвеладзе А.С., Соломин Д.А., Васильев И.Ю. [Модификация полимерных композиций с термопластичным крахмалом для биоразлагаемой упаковочной пленки](#): В книге: Биотехнология: состояние и перспективы развития. Материалы международного конгресса. 2019. С. 102-104.
17. Колпакова В.В., Усачев И.С., Сарджвеладзе А.С., Соломин Д.А., Ананьев В.В., Васильев И.Ю. [Совершенствование технологии применения термопластичного крахмала для биоразлагаемой полимерной пленки: Пищевая промышленность](#). 2017. № 8. С. 34-38.

18. Ananyev V.V., Nagornova I.V., Bablyuk E.B., Vasilyev I.Y., Varepo L.G. [Polymer composites including natural additives degradation rate indication](#). В сборнике: AIP Conference Proceedings. 2017. С. 020091.
19. Thermoplastic composition with modified porous corn starch of biodegradability properties / Kolpakova V., Usachev I., Papakhin A., Sardzhveladze A., Ananiev V. // International conference on geosciences. 2019.- 26-29.03.-. Athens, Greece.
20. Лукин Н.Д., Колпакова В.В., Усачев И.С., Папахин А.А., Сарджвеладзе А.С., Бородина З.М., Васильев И.Ю., Ананьев В.В. [Биологически разрушаемая термопластичная композиция](#). Патент на изобретение RU 2691988 C1, 19.06.2019. Заявка № 2018146738 от 26.12.2018.
21. Васильев И.Ю., Ананьев В.В., Колпакова В.В., Сарджвеладзе А.С. [Разработка технологии получения биоразлагаемых композиций на основе полиэтилена, крахмала и моноглицеридов. Тонкие химические технологии](#). 2020. Т. 15. № 6. С. 44-55.
22. Усачев И.С., Сарджвеладзе А.С., Васильев И.Ю., Соломин Д.А. [Совершенствование технологических режимов производства биоразлагаемых полимерных пленочных изделий методом экструзии](#). В сборнике: Перспективные исследования и новые подходы к производству и переработке сельскохозяйственного сырья и продуктов питания. Сборник научных трудов XIII Международной научно-практической конференции молодых ученых и специалистов организаций в сфере сельскохозяйственных наук. 2019. С. 348-353
23. L. A. Wasserman, A. A. Papakhin, Z. M. Borodina [et al.] / Some physico-chemical and thermodynamic characteristics of maize starches hydrolyzed by glucoamylase // Carbohydrate Polymers. – 2019. – Vol. 212.– P. 260–269. DOI: <https://doi.org/10.1016/j.carbpol.2019.01.096>.
24. Kwon, S. S. Physicochemical properties of pH-sensitive hydrogels based on hydroxyethyl cellulose-hyaluronic acid and for applications as transdermal delivery systems for skin lesions / S. S. Kwon, B. J. Kong, S. N. Park // European Journal of Pharmaceutics and Biopharmaceutics. – 2015. – Vol. 92. – P. 146–154. DOI: <https://doi.org/10.1016/j.ejpb.2015.02.025>.
25. Razavi, S. M. A. Structural and physicochemical characteristics of a novel water-soluble gum from Lallemania royleana seed / S. M. A. Razavi, S. W. Cui, H. Ding // International Journal of Biological Macromolecules. – 2016. – Vol. 83. – P. 142–151. DOI: <https://doi.org/10.1016/j.ijbiomac.2015.11.076>.

INOVACIJOS LEIDYBOS, POLIGRAFIJOS
IR MULTIMEDIJOS TECHNOLOGIJOSE 2021
Konferencijos straipsnių rinkinys

International scientific-practical conference
INNOVATIONS IN PUBLISHING, PRINTING
AND MULTIMEDIA TECHNOLOGIES 2021
Conference proceedings

ISSN 2029-4638

Spausdino Kauno kolegijos leidybos centras,
Pramonės pr. 20 LT-50468 Kaunas
Maketavo *Virginijus Valčiukas*
Tiražas 40. Užsakymo Nr. I-2383